ELSEVIER

Polymer 41 (2000) 285–310

polymer

Surfactant level influences on structure and properties of flexible slabstock polyurethane foams

B.D. Kaushiva[a], S.R. McCartney[a], G.R. Rossmy[b], G.L. Wilkes[a,*]

[a]*Polymer Materials and Interfaces Laboratory, Department of Chemical Engineering, Virginia Polytechnic Institute and State University, Blacksburg, VA 24061-0211, USA*

[b]*Im Hadkamp 18, D-45721 Haltern-Lavesum, Germany*

Received 1 November 1998; received in revised form 11 January 1999; accepted 11 January 1999

Abstract

A series of flexible polyurethane slabstock foam samples were prepared with varying surfactant concentration. Several samples were also prepared by quenching small pieces into liquid nitrogen during the foaming process. The morphology of these materials was characterized at many length scales via scanning electron microscopy (SEM), transmission electron microscopy (TEM), wide-angle and small-angle X-ray scattering (WAXS and SAXS), tapping-mode atomic force microscopy (AFM), and Fourier transform infrared spectroscopy (FTIR). AFM was also utilized to probe trends in the mechanical stiffness of hard domains in the polyurethane foam. Differential scanning calorimetry (DSC) and dynamic mechanical analysis (DMA) were applied to examine the thermal and viscoelastic properties of these foams. It was shown in this study that collapse of the cellular structure of a foam prior to the point of urea precipitation alters the aggregation behavior of the hard domains and influences their ultimate properties. Samples without surfactant quenched in liquid nitrogen exhibited urea-rich aggregations on the order of 2–4 μm with similar sized urea-poor regions. Equivalent samples with surfactant showed no such aggregations, suggesting that surfactant does play a principal role in the way that urea precipitates in these materials. DMA and DSC revealed that all samples of any surfactant concentration which spontaneously collapsed or were quenched or crushed prior to completely curing had a polyol glass transition 3–5° higher and somewhat broader than any foam sample which maintained its cellular structure until cured. This is interpreted to mean that the polyol matrix of the collapsed, crushed, or quenched materials is not as pure as the cellular samples, indicating that the presence of the cellular morphology plays a significant role in the microphase separation behavior of the solid-state at the molecular level. This hypothesis is supported by the results of WAXS, FTIR, SAXS, and AFM. The WAXS results demonstrate that at no surfactant concentration is the ordering, or hydrogen bonding, within the hard domains being significantly altered; however, in the lower range of the concentrations studied here, the FTIR results show that the surfactant level in the formulation does play a significant role on the amount of bidentate hydrogen bonded hard domains that organize locally. Further, as shown by SAXS, the surfactant concentration influences the mean chord length across the hard domains. These changes in structure and domain size distribution lead to the properties investigated via AFM, where the relative hardness of the hard domains was noted to initially increase as the surfactant concentration increases and then levels off above a certain concentration. The surfactant is thus suggested to play a secondary role in the development of the hard domains by maintaining the cellular structure in the foam as the phase separation occurs and at least until the polyurethane foam has more fully organized hard segment domains.

Keywords: Polyurethane; Foam; Surfactant

1. Introduction

The two-phase morphology of the solid state is of great importance to overall properties in polyurethane foams. In typical water-blown systems, the reaction of water with diisocyanate produces a carbamic acid which decomposes yielding heat, carbon dioxide, and an amine functionality [1]. The heat and carbon dioxide contribute to the expansion of the gas–liquid phase separation in the reactive mixture and so play important roles in the development of the foam's cellular structure. However, a disubstituted urea product results from the reaction of the amine with other isocyanate groups. A "hard segment" results from several isocyanate groups covalently bonding through the urea linkages, and solid-state phase separation in typical systems arises from the precipitation of these segments into "hard domains." In conventional flexible slabstock foams, the polyol phase has a very low T_g (ca. −50°C) and so is

* Corresponding author. Tel.: + 1-540-231-5498; fax: + 1-540-231-9511.

E-mail address: gwilkes@vt.edu (G.L. Wilkes)

0032-3861/00/$ - see front matter
PII: S0032-3861(99)00135-4

often termed "soft." The soft polyol is generally thought to be the continuous phase in these systems, and it is considered to be the matrix in which the hard domains are distributed. However, as will be discussed in detail later, some studies in mechanical deformation and hard segment orientation have suggested that there may be some degree of association or connectivity between hard domains that cannot be explained from the fully dispersed hard domain model. Ideally, hard segments are covalently bound to the polyether polyol during the reaction of the polyol with isocyanate groups, which lead to urethane linkages at their terminal points. However, it is known that in real systems there is a distribution of urea segment lengths and that some hard segments are incompletely bound to the polyol matrix [2].

An additional structure is also sometimes observed in these systems. At high water feed concentration with a stoichiometrically higher feed of isocyanate, the urea precipitates can aggregate further to form what have been termed "urea balls" or urea-rich aggregates [1,3]. These larger aggregates are frequently observed in conventional slabstock flexible foam formulations of high water concentration; however, these structures are not typically observed in molded or high-resiliency (HR) foams of the same water feed concentration [1,4,5]. This difference results from the chemistry of the typical components used in each. Whereas both molded (HR) and slabstock flexible foams most commonly utilize toluene diisocyanate or TDI (fed at an 80/20 2,4/2,6 isomer ratio), the polyol used for each is one major formulation difference. Typical slabstock polyols have molecular weights between 3000 and 4000 Da; molded polyols tend to have higher molecular weights in the range of 4000–6000 Da [1]. Both systems utilize polyether triols; however, the ethylene oxide (EO) to propylene oxide (PO) ratio of each is generally very different. Slabstock foams tend to use lower EO content and have secondary OH endgroups. To achieve faster reaction rates, molded systems most frequently have much higher ethylene oxide content, and they use polyols with primary OH content in the range of 65–90% [1]. The faster reaction rate requires a different blend of catalysts as well as lower potency surfactants to obtain an open celled foam. Also, increasing the EO content of the polyol dramatically alters the miscibility of water and other reaction components; further, it is believed that variation of the EO/PO ratio also has profound effects on the solubility of the hard segments in the polyol matrix of the final foam [1]. It is therefore deduced that the larger aggregates (urea balls) may form as either the hard segments or the urea precipitates or some combination of both reach a size or a concentration that surpasses a solubility limit which varies depending on the chemical system being utilized [1,3].

As the polyol usually has a functionality between two and three, these systems promote a covalent network. However, the development of hydrogen bonding of the hard segments as they precipitate also forms a network based on physical associations. The mechanical nature of that network is highly dependent on the shape of the polyurea precipitates. For instance, in a system of dispersed spheroids, each of these urea-based domains would behave as a physical crosslink; however, if the precipitates develop in a more lamellar-like fashion, a co-continuous network might form instead. In summary, these systems are composed of at least two solid state phases and two types of "crosslinks," chemical and physical. A more specific review of these structures is available in Refs. [4,6]. It should be made clear that although the hydrogen bonds provide the physical crosslinks with cohesive strength, they are not themselves the crosslinks. This hydrogen bonding between hard segments leads to a partially ordered or to a possibly "para-crystalline" texture which will be discussed more later in this article. It should also be stated that the hydrogen bonding in a hard domain or urea precipitate is believed to be of the same type as that found in the hard domain aggregates or urea balls. Initial X-ray microscopy work by Ade et al. [7] on diphenylmethane diisocyanate (MDI) based foams has shown that these urea balls are not entirely urea but do contain some polyol. As yet unpublished work by Ade [8] on TDI based foams, more similar to typical slabstock formulations like those used in this study, has shown that although these large aggregates still consist mainly of urea linked TDI they also contain ca. 5–10% polyol in the center with increasing amounts away from the center of the urea ball. This strongly indicates that the large aggregates are not entirely urea based hard segment material but may be thought of as aggregations of precipitates.

In examining how these materials behave during mechanical deformation, workers [9] have shown hard segment orientation transverse to the direction of elongation in flexible slabstock foams followed by additional orientation parallel to the stretch direction. This somewhat surprising behavior, also noted first in polyurethane elastomers, can best be explained by suggesting that hard domains associate with one another to form lamellar-like structures which then dissociate under shear yielding and rupturing on further elongation [9,10]. This behavior suggests structure on a larger scale rather than the interdomain distances typically observed via small-angle X-ray scattering (7–11 nm). This indicates that such spacings may be the distances between lamellar-like formations, and that much larger lateral dimensions of the lamellae exist. However, no well-defined lamellar-like structure in polyurethane foams has ever been distinctly and unambiguously observed via microscopy [6]. This discussion brings up the question of how well dispersed the hard domains actually are in polyurethane foams. Connectivity between them or associations on a scale larger than the size of hard domains could well lead to the behavior observed in Ref. [9]. It should be obvious from this discussion that, whether in more localized urea-based hard segment domains or in larger urea aggregates, association via hydrogen bonding provides ordering that is of great importance to understanding the properties of these polymers.

Previous studies have demonstrated that many factors can influence the hard domain ordering, and that these can have large impacts on the properties of flexible polyurethane foams [4–13]. Humidity and temperature have both been shown to increase the rate of stress relaxation and compressive load relaxation [4,11]. These variables have also been shown to have an influence on compressive creep behavior [12,13]. It has also been demonstrated that cyclic humidity conditions increase the amount of compressive creep relative to samples held at a constant humidity [13]. These studies were performed over a few hours in the thermal range between room temperature and 100°C, generally too low for polymer decomposition on those time scales. It is therefore widely accepted that the thermal dependence is a result of the weakening of the hydrogen bond associations of the hard segments. This hypothesis is supported by the parallel humidity dependence because the polyol is largely hydrophobic and the urea domains are more hydrophilic [13]. These observations indicate the strength of the dependence of foam properties on the hard domains.

If foam properties are so dependent on the hard domains, it might be anticipated that variables which influence the concentration, composition, distribution, or ordering of the hard domains would thus become important to the final foam. These effects have in fact been demonstrated by many studies [14–17]. Hard segment content can be varied in foams by stoichiometrically increasing water and isocyanate in the feed while maintaining the amount of polyol added. In a work by Turner et al., thus increasing hard segment content at constant soft segment content was shown to significantly increase the rubbery modulus of the foam [14]. This confirms that changing hard segment concentration can dramatically alter viscoelastic properties as would be expected. The importance of hard domain composition in foams has been shown by a study that incorporated the cross-linking agent diethanol amine (DEOA) into the foam formulation [15]. DEOA had the effect of altering the composition of the hard segments, and thereby dramatically changing their hydrogen bonding associations. This change in composition increased the lability in the hard domains, making them more susceptible to water and thermal “plasticization”. Additionally, the use of lithium chloride as a property modifier has been shown to soften the foam by disrupting hard domain ordering as noted by wide-angle X-ray scattering (WAXS) and altering their distribution in the matrix as revealed by small-angle X-ray scattering (SAXS) and by solid-state NMR [16,17].

The above cases only relate the importance of hard domains to the overall properties of a foam. However, it has also been determined that the precipitation of urea is an important event in the development of foam structure [18,19]. Foams without surfactant have been observed to be stable up to the point of urea precipitation—after which point they collapse [20]. More recent work on molded foam formulations using MDI rather than TDI have shown that, although urethane and urea linkages form immediately in the reactive mixture, the precipitation of urea groups occurs later, an event which leads to cell opening [21]. This precipitation behavior is thus vital to understanding the formation of a mechanically sound, open-celled foam.

Polysiloxane–polyether block copolymers of various topologies are used as surfactants in foams to stabilize the developing cell structure. In most formulations, stabilization is needed until gelation occurs through chemical crosslinking from the reaction of polyol with isocyanate, and this stabilization can prevent urea precipitation from collapsing the foam upon cell opening. As precipitation of hard segments into hard domains occurs, they organize via hydrogen bonding forming physical crosslinks; moreover, it has been observed that this phenomenon parallels dramatic increases in the modulus of the material [21].

The importance of stabilizing the dispersion of the urea precipitates is underscored by the earlier work of Rossmy et al. [20] *wherein foams were made with only surfactant, catalysts, water, and isocyanate (i.e. no polyol*). In that work, three surfactants were used based on the same polysiloxane blocks but with polyether blocks varying in molecular weight and ethylene oxide/propylene oxide ratio. The first surfactant, using a polyether component of only propylene oxide with a molecular weight of 1800, was incapable of maintaining the dispersion without the presence of polyol crosslinking, and with this surfactant the foam collapsed immediately following cell opening. The second surfactant used a polyether component of 45 wt.% ethylene oxide and a molecular weight of 1500, and this second foam also collapsed following cell opening. In contrast, the third surfactant, which also did not have the benefit of polyol covalent crosslinking, did maintain the dispersion and formed a stable, open-celled foam. This last surfactant utilized a polyether block of 45 wt.% ethylene oxide and a molecular weight of 2000. These studies thus indicate that some formulation dependent combination of surfactant stabilization and covalent crosslinking is necessary to prevent urea precipitates from aggregating to sizes that promote collapse of the foam. This shows that, whereas organized urea precipitates provide the necessary modulus for good mechanical properties, *the dispersion of those precipitates throughout the polymer matrix promoted by surfactant stabilization or covalent crosslinking is necessary in maintaining an open celled foam structure*. This work also points out the crucial role that ethylene oxide can play in polyurea stabilization whether it is used in surfactants or for endcapping polyols as is done in many molded foam formulations.

Recently, Yasunaga et al. [22] have further explored the event of cell opening in flexible slabstock foams. One result of that study confirmed the conclusions of Elwell et al. [21] wherein the storage modulus development in foams follows the events of urea precipitation and cell opening. This further establishes the hypothesis that the organization of the hard domains is the driving factor in increasing mechanical properties. However, it also speaks of the importance of

Table 1
Sample designations and their meanings

Sample name	Comments
SSu0.0	Slabstock foam, 0.0 surfactant pphp
SSu0.3	Slabstock foam, 0.3 surfactant pphp
SSu0.75	Slabstock foam, 0.75 surfactant pphp
SSu1.5	Slabstock foam, 1.5 surfactant pphp
SSu10.0	Slabstock foam, 10.0 surfactant pphp
SSu20.0	Slabstock foam, 20.0 surfactant pphp
Q100-Su0.0	Quenched at 100 s, 0.0 surf. pphp
Q100-Su1.5	Quenched at 100 s, 1.5 surf. pphp
Q120-Su0.0	Quenched at 120 s, 0.0 surf. pphp
Q120-Su1.5	Quenched at 120 s, 1.5 surf. pphp
C80-Su1.5	Mechanically crushed at 80 s, 1.5 surf. pphp
C106-Su1.5	Mechanically crushed at 106 s, 1.5 surf. pphp
ShiEO	High ethylene oxide content slabstock
UPA	Urea powder (TDI/H_2O) made in acetone
UPSu	Urea powder (TDI/H_2O) made in surfactant
MD0.0	Molded foam with 0.0 deoa pphp
MD2.0	Molded foam with 2.0 deoa pphp

understanding the initial event of urea precipitation. Yasunaga et al. [22] also confirmed the earlier study of Rossmy et al. [18] in that increasing the surfactant concentration slows the rate of foam expansion and lengthens the time to cell opening. *The implication of this is that surfactant concentration has an influence on the precipitation of the urea and therefore may have an influence on the microphase behavior of the final polymer material comprising the foam, possibly by altering the shape, size, or the distribution of the urea precipitates*.

Given the voluminous use of polyurethane foams and the dependence of their properties on these hard domains, it can be seen that it would be valuable to better understand their structural development and properties. As discussed above, although the surfactant is known to influence the rate of foam development and is hypothesized to influence urea precipitation behavior, this relationship is not well understood. Therefore, rather than study how the topology and composition of a surfactant influences foam stabilization, this study seeks to understand how surfactant influences microphase morphology by choosing one widely used surfactant [1,6] and studying how varying its concentration in a series of slabstock foams alters solid state phase behavior.

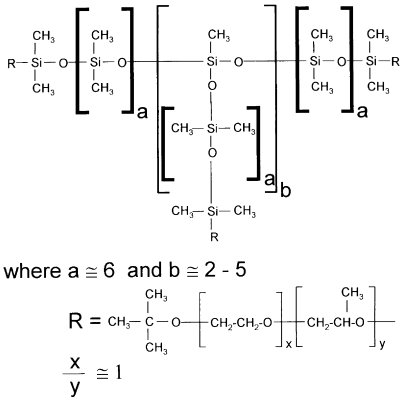

Fig. 1. Structure of Tegostab® BF 2370 (Goldschmidt AG). Average molecular weight for the copolymer is 8 800. There are no emulsifying ingredients present in the surfactant besides remaining monol residues of the polyether mixture used for the copolymer synthesis.

2. Experimental materials and methods

2.1. Materials

Several foam samples of flexible water-blown polyurethane foams were made with varying surfactant concentrations. These foams were based on 100 parts of Voranol® CP 3322 (Dow Chemical), a triol containing 88% propyleneoxide and 12% ethyleneoxide with terminal secondary OH-groups. The foams also used 4 parts of water and TDI 80 (an 80/20 mixture of the 2,4/2,6 isomers) fed at an isocyanate index of 105. Dimethylethanolamine was used as a catalyst for the water-isocyanate reaction at a concentration of 0.2 pphp (parts per hundred polyol). Stannus octoate was used as a polyol-isocyanate reaction catalyst also at 0.2 pphp. A widely used surfactant for slabstock foams, TEGOSTAB® BF 2370 (Goldschmidt), was selected for this study, and it was varied as shown in Table 1. The nomenclature in Table 1 is completely explained at the end of this section. The structure of this surfactant is shown in Fig. 1. (Six foams were made that were allowed to develop fully with an additional 15 min cure at 140°C to remove tackiness.)

To explore the development of polymer morphology, four foams were quenched in liquid nitrogen at specific times during the foam reaction, two at 100 s and two at 120 s. Blow-off time for these formulations generally occurred at 110 s, so these quench times were picked to bracket that event. Two surfactant-containing foams were also mechanically compressed to examine possible influences that the removal of cellular structure may have on the development of microphase separation in the solid state. One of these was crushed at 80 s, the time at which the 0.0 surfactant pphp foam spontaneously collapsed. The other foam was crushed at 106 s, the rise time to final height for that foam formulation. For all six of these samples, small quantities of material were taken from the reacting foam and then quenched or crushed. This was done to assure that the entire sample had a uniform thermal and morphological history characteristic of their respective times of quenching or crushing.

For general comparisons, one additional foam was prepared specifically to reduce urea particle precipitation into hard domains. This formula was based on 75 parts of polyol ™Desmophen 7040 with an ethylene oxide content of 75% and 25 parts of polyol ™Desmophen 7160 with an ethylene oxide content of 12%. This formula used 2.0 surfactant pphp, 3.8 water pphp, and 0.3 amine catalyst (™Dabco) pphp. This formula also used a TDI 80 at an

Table 2
Some relevant IR absorbances

Resonating group	Wavenumber (cm^{-1})
Free urethane	1730
Free urea	1710–1715
Hydrogen bonded urethane	1705–1700
Monodentate urea	1700–1650
Bidentate urea	1640–1650

isocyanate index of 95. Finally, two polyurea-based powders were produced. One was made by dissolving TDI 80 in acetone and slowly feeding in an excess of water to produce polyurea segments with a calculated number average of 10 repeat units. The acetone was evaporated and the powder was then dried in a vacuum oven. The other powder was produced by using the same formula as the slabstock foams but replacing all of the polyol with ™TEGOSTAB BF 2370 (Goldschmidt) [23].

The nomenclature for these samples is as follows. Generally, the first letter of a sample name indicates the type of sample and the manner in which it was made. The next set of letters indicates what the variable was for that sample. For instance, SSu0.0 is a slabstock foam in which the surfactant concentration was 0.0 pphp. Possible first letters include: "S" for a slabstock foam; "M" for a molded foam (two molded foams were utilized for comparative WAXS and Fourier transform infrared spectroscopy (FTIR) analyses); "C" for a foam that was crushed; "Q" for a foam that was quenched in liquid nitrogen; and "UP" for a polyurea powder. Numbers are included for the letter of the variable that they follow. As used above, it gives the concentration of surfactant in a sample. In Q100-Su0.0 or C80-Su0.0, the 100 or 80 corresponds to the time in seconds after the foam reactions were initiated that the samples were quenched or crushed, respectively. Finally, there are three exceptions to this nomenclature. SHiEO is the slabstock foam made with the high ethylene oxide content polyol discussed. UPA and UPSu are polyurea powders made in pure acetone and pure surfactant, respectively.

3. Methods

Dynamic mechanical analysis (DMA) was carried out using a Seiko model 210 in the tension mode. The samples were heated from −120°C to 350°C at a rate of 0.5°C/min. from which the storage modulus (E') and tanδ data were collected at a frequency of 1 Hz. Samples were cut from the foam with die-punches and had dimensions of approximately 5 × 5 × 15 mm with a grip-to-grip distance of 10 mm. Storage moduli are normalized to 3×10^9 Pa to remove the effect of varying density which is only a function of the cellular structure [14]. Differential scanning calorimetry (DSC) was performed on a Seiko model DSC 220C. Scanning at 10°C/min from −120 to 350°C. This was performed for comparison with the tanδ data from the DMA.

SAXS was utilized to evaluate the presence of microphase separation. This was performed with a Phillips model PW1729 generator operating at 40 kV and 20 mA and a slit collimated ($0.03 \times 5\ mm^2$) Kratky camera with nickel filtered CuK_α radiation having a wavelength of 1.542 Å. The detector utilized was a Braun OED 50 position-sensitive platinum wire detector. Scattering data were corrected for parasitic scattering and normalized using a Lupolen standard. As the apparent density varied, the beam path length for the non-quenched and non-crushed foam samples ("S" series in Table 1) was also corrected based on the density relative to the apparent density of sample C80-Su1.5. The foam samples were cut approximately 8 mm thick and compressed to approximately 2 mm. These data were analyzed using the TOPAS program developed by Dr Stribeck at the University of Hamburg. Dr Stribeck has graciously posted TOPAS for free downloading on the World Wide Web at "http://www.chemie.uni-hamburg.de/tmc/stribeck/index.html".

To explore the ordering of the hard domains, the technique of WAXS was applied via a Phillips model PW1720 generator with a Warhus camera. Nickel filtered CuK radiation was used with a wavelength of 1.542 Å and pinhole collimation with a diameter of 0.020 in. These samples varied widely in apparent density; therefore, using their apparent density and the 0.020 in. beam diameter as a basis for the calculation, samples were cut to thickness which would expose ca. 3.2 mg of material to the beam. Foam samples were compressed to a ca. 2 mm thickness, but the collapsed materials did not need this compression. Sample to film distance was 7.7 cm and exposure times were ca. 10 h.

FTIR was also used to evaluate hydrogen bonding in the hard domains as shown in Table 2 [24]. FTIR Spectra were collected on a Nicolet 510 Spectrometer using a Spectra-Tech ATR attachment. The ATR cell utilized a horizontal ZnSe crystal. Spectra were analyzed using OMNIC 3.0 software, and all scans were normalized by the corrected peak height at 2970 cm^{-1} which corresponds to a CH_3 absorbance [18].

Characterization of the cellular structure of the foam was performed with scanning electron microscopy (SEM). Thin foam slices, ca. 5 mm, were mounted to aluminum stubs using copper tape. These samples were then sputter coated with gold to ca. 15 nm thickness. Micrographs were taken using a Cambridge Stereoscan model 200 operating at 10 kV and at magnifications of ca. 100 ×.

Transmission electron microscopy (TEM) was used to observe the precipitated urea particulate. Small samples were cut from the foams and then embedded in epoxy which cured at 60°C overnight. Thin sections (ca. 80 nm) were then cryogenically microtomed using a diamond knife on a Reichert-Jung Cryo-ultramicrotome Ultracut E with a model FC-4D cryo-attachment operating at −90°C. Ethanol

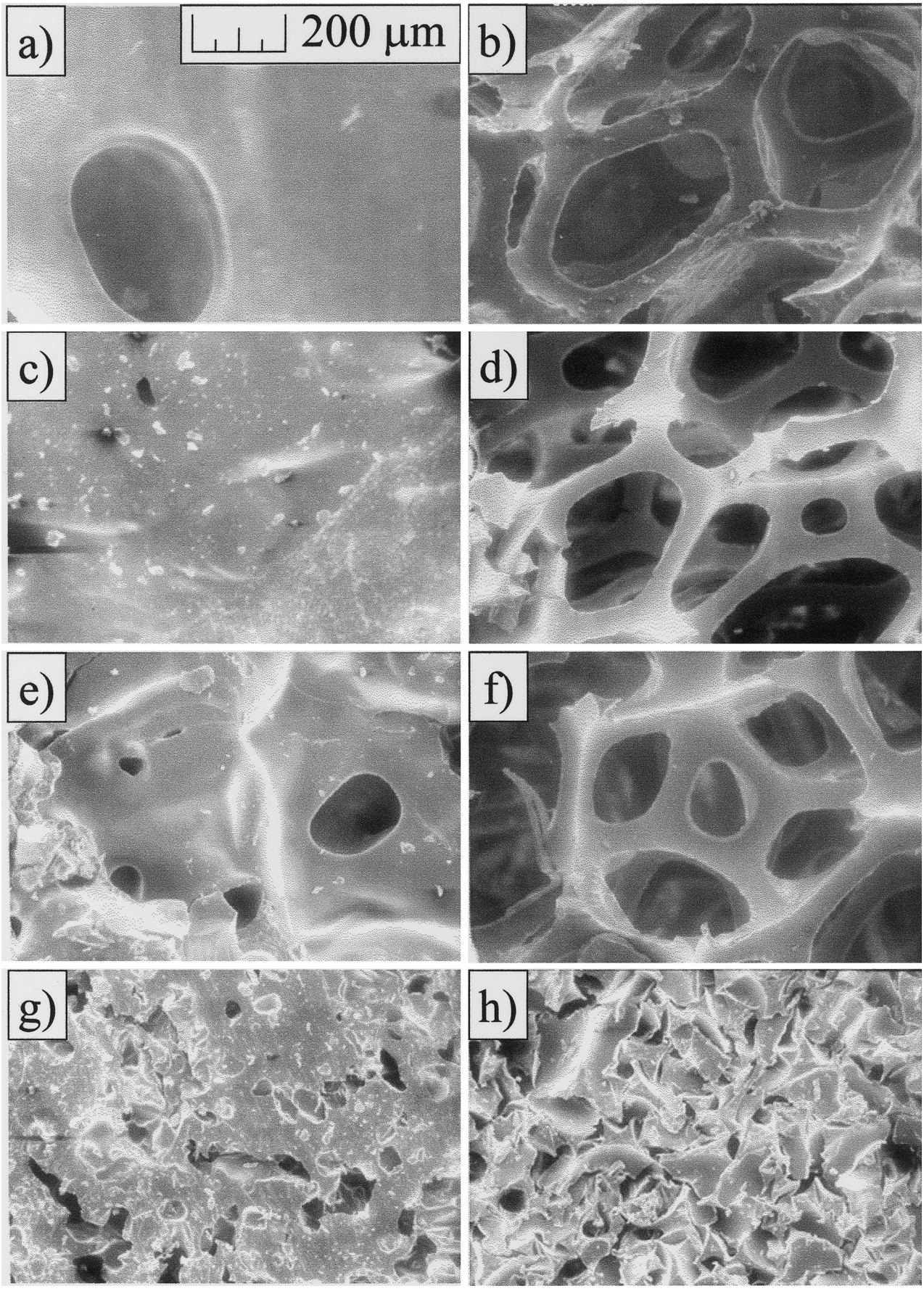
a)
200 μm
b)
c)
d)
e)
f)
g)
h)

Table 3
Apparent densities of the samples

Sample name	Apparent density (g/cm3)
SSu0.0	0.1810
SSu0.3	0.0260
SSu0.75	0.0234
SSu1.5	0.0245
SSu10.0	0.0226
SSu20.0	0.0265
Q100-Su0.0	0.3978
Q100-Su1.5	0.3225
Q120-Su0.0	0.0332
Q120-Su1.5	0.0590
C80-Su1.5	0.7446
C106-Su1.5	0.3536
ShiEO	0.0232

was used to collect the sections onto 600 mesh copper grids. Micrographs were taken using a Philips 420T scanning transmission electron microscope (STEM) operating at an accelerating voltage of 80 kV. Micrographs were taken at three levels of magnification, corresponding on the negatives to 37 500 ×, 10 500 ×, and 3300 ×.

Atomic force microscopy (AFM) in tapping mode was also used to study nanoscopic level structure. These experiments were performed on a Digital Instruments Scanning Probe Microscope using Nanosensors TESP (Tapping Etched Silicon Probe) type single beam cantilevers. These cantilevers had nominal lengths of ca. 125 μm, force constants of approximately 35 ± 7 N/m, and were used at oscillation frequencies at ca. 290 kHz. The samples mounted in epoxy for TEM were cryo-microtomed smooth and then examined by AFM. The phase image of AFM is generated by recording the phase shift that occurs between the drive oscillation on the cantilever and the oscillation of

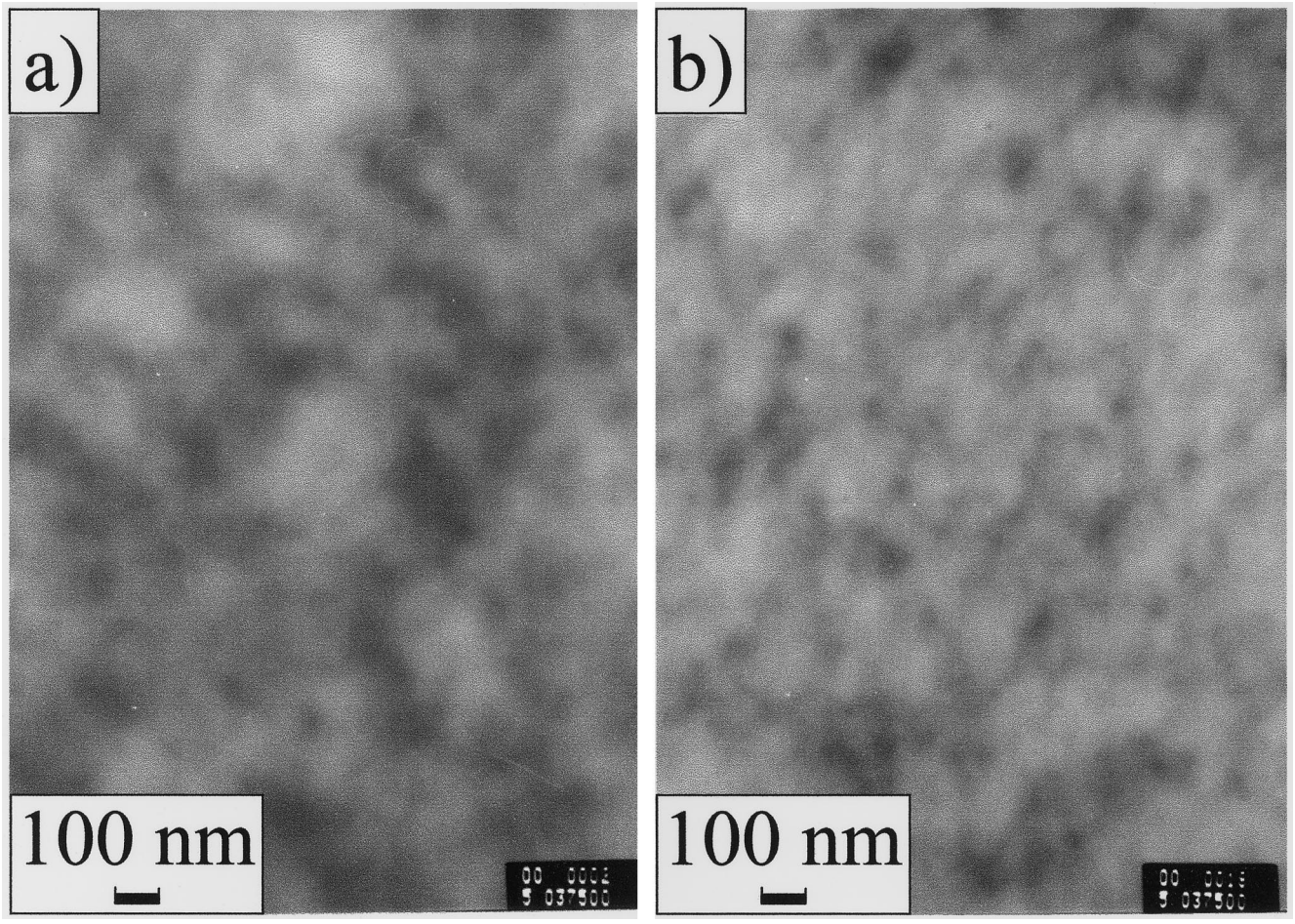

Fig. 3. Transmission electron high magnification micrographs for two foams with varying surfactant concentration: (a) SSu0.0 and (b) SSu1.5.

Fig. 2. Scanning electron micrographs of foams in various states: (a) SSu0.0; (b) SSu1.5; (c) Q100-Su0.0; (d) Q100-Su1.5; (e) Q120-Su0.0; (f) Q120-Su1.5; (g) C80-Su1.5; and (h) C106-Su1.5. The scale bar shown in 2a) applies to all of the micrographs.

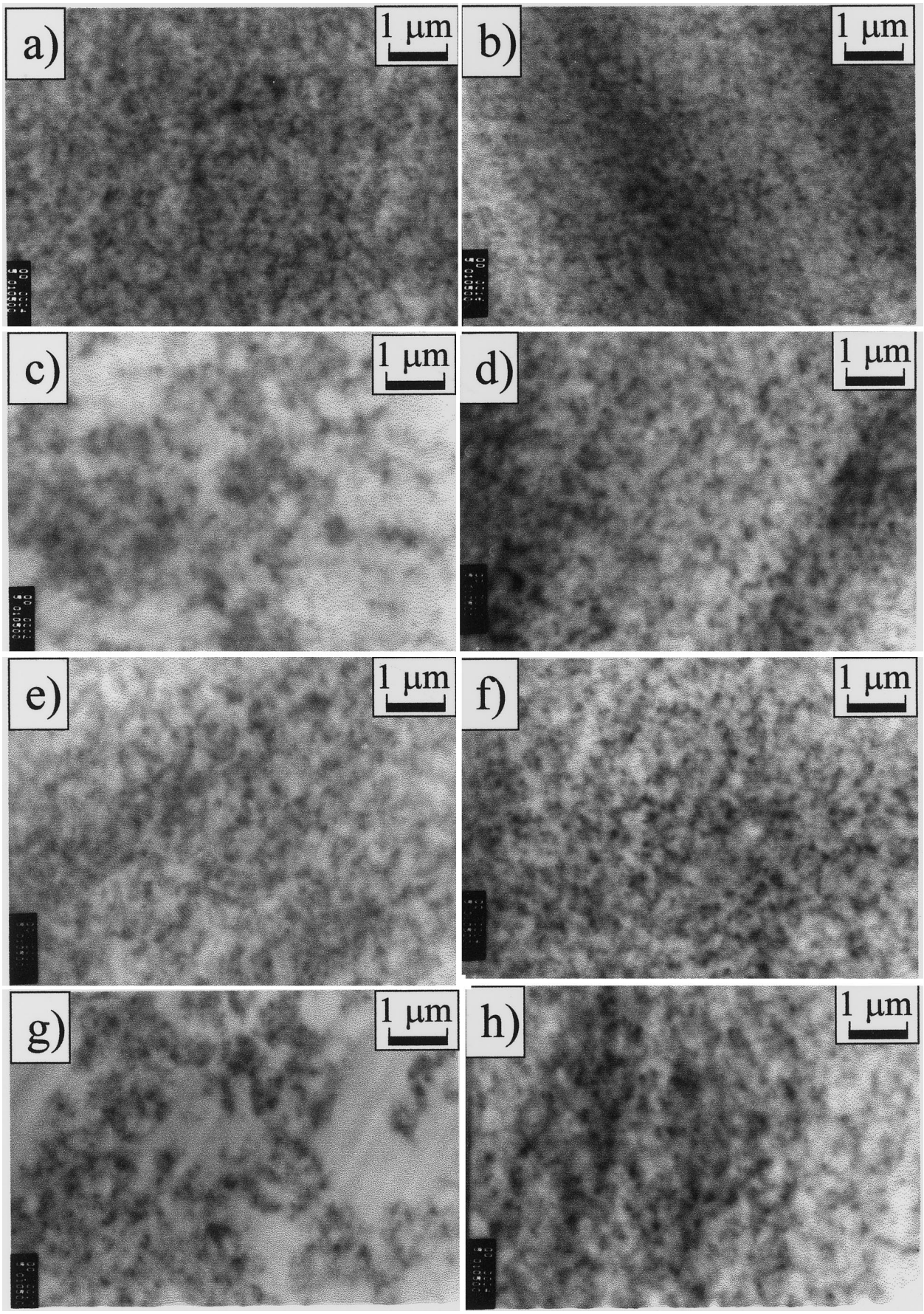
a)
1 μm
b)
1 μm
c)
1 μm
d)
1 μm
e)
1 μm
f)
1 μm
g)
1 μm
h)
1 μm

the cantilever tip. The phase shift of a cantilever oscillating in free air would be close to zero. As the oscillating tip contacts the surface its phase shift is relative to the interactions occurring between tip and sample. Phase shift becomes more positive when interacting with harder materials, and estimations from the Hertz theory lead to the relation that phase shift scales with the dynamic modulus of the sample [25]. It should also be pointed out that once AFM phase images using scales above 1 or 2 μm are saved much information on the scale lengths of the hard domains (ca. 7–11 nm) is lost. Thus, to obtain and later analyze the high resolution information needed regarding the phase offset, phase images measuring 2 μm × 2 μm were collected for quantitative analysis. Further details on phase imaging with tapping mode AFM are available online at "http://www.digital.com/AppNotes/Phase/PhaseMain.html".

A series of AFM experiments were used wherein the force applied to the surface was controlled by holding two variables constant. The amplitude of the cantilever's free air oscillation was maintained at 5.05 V. However, as the tip oscillates, its amplitude while striking the surface is lower than that value and was maintained at 60% of the value of the free air amplitude. Control of these two factors should maintain constant the energy of the cantilever as well as the force being applied to the surface. By randomly sampling the surfaces, by using new tips, and by scanning surfaces multiple times, reproducible levels of maximum phase offset were observed. These values are used in this work to follow trends regarding the *relative hardness* of the hard domains. This effect has been recently been qualitatively shown in triblock copolymers and polyurethane elastomers by McLean and Sauer [26]. Further, this technique was first demonstrated by application to flexible polyurethane foams by the authors in a previous publication [27]. This work will also seek to further quantify these efforts.

4. Results and discussion

To understand the influence of surfactant on properties, its effect upon morphology must also be understood. It is well known that without surfactant, the cellular structure collapses before the gelation reaction can stabilize the foam [1]. This can be observed in Fig. 2a–h where eight SEM micrographs show the typical pattern of cellular structure observed in this study.

Fig. 2a reveals that the morphology of SSu0.0 might be characterized as large gas pockets held within wide, voidless polymeric regions. Fig. 2b shows that SSu1.5 has the cellular structure expected in a slabstock foam with cell diameters greater than 1 mm. This cellular morphology was observed at all surfactant concentrations examined greater than zero. Fig. 2c and d compare the structure of the quenched foams, Q100-Su0.0 and Q100-Su1.5. It is observed that, even in these incompletely reacted foams, the difference made by the presence of the surfactant is apparent. Q100-Su0.0 shows a very smooth surface compared to Q100-Su1.5 which exhibits smaller (<1 mm diameters) but recognizable cells "frozen" in their nascent state. The micrographs of samples Q120-Su0.0 and Q120-Su1.5 are presented in Fig. 2e and f, and it can be seen that they exhibit similar behavior to samples Q100-Su0.0 and Q100-Su1.5, respectively. Fig. 2g reveals that sample C80-Su1.5 resembles the morphology of samples Q100-Su0.0 and Q120-Su0.0 in that it is not composed of cells but of a continuous polymer matrix with some gas bubbles spread throughout it. It is noted, however, that this sample has many more gas pockets than any of the Fig. 2c–f. However, the small amount of gas present in sample C80-Su1.5 is demonstrated by the apparent densities of the samples listed in Table 3. It is shown there that this crushed sample has half as much gas as the other collapsed specimens.

Fig. 2h reveals that C106-Su1.5 has very different morphology. This crushed foam is composed of pieces of the cellular structure observed in Figs. 2f or 2d squeezed together. It seems that just after cell opening at 106 s, the foam has achieved enough dimensional stability to prevent congealing to the extent seen in Fig. 2g. This sample and sample C80-Su1.5 will then be used to evaluate the importance of the presence of the cellular structure to the organization of the hard domains at the point of urea precipitation. Further, these micrographs illustrate that, without surfactant, the reactive mixture has relatively little surface area of a gas–liquid interface in comparison to mixes with surfactant. It also shows that with surfactant the larger surface area may be altered by crushing or quenching, but it is still clearly present.

TEM was used to evaluate the solid morphology within the cell wall material itself. This technique has been used in other studies [6] to examine larger scale precipitation behavior of the urea which shows up as dark regions in the micrographs. At the highest magnifications used, the two micrographs of Fig. 3 examine the size of the urea rich aggregations. Fig. 3a shows that in SSu0.0 the precipitates begin around 100 nm in diameter and get larger. Fig. 3b reveals, however, that in SSu1.5 precipitates begin around 100 nm in diameter and get smaller. While these are subtle size differences, they are representative and, further this subtle difference will be supported by other results. Further, this may be one sign of alterations in the distribution of urea precipitates in the matrix. It may indicate that what connectivity may be developing occurs via associations between

Fig. 4. Transmission electron medium magnification micrographs of foams in various states: (a) SSu0.0; (b) SSu1.5; (c) Q100-Su0.0; (d) Q100-Su1.5; (e) Q120-Su0.0; (f) Q120-Su1.5; (g) C80-Su1.5; and (h) C106-Su1.5.

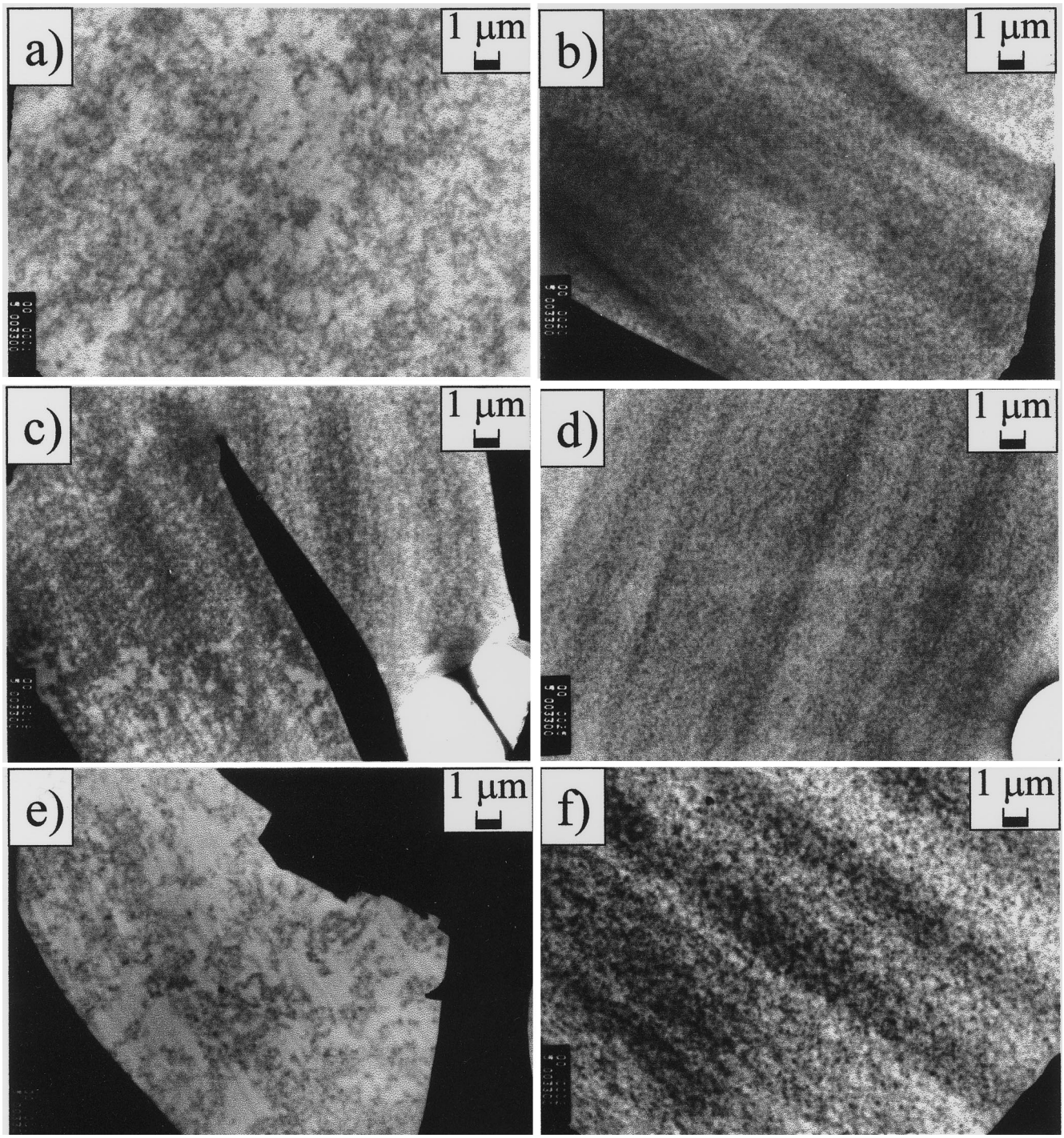

Fig. 5. Transmission electron low magnification micrographs of foams in various states; (a) Q100-Su0.0; (b) Q100-Su1.5; (c) Q120-Su0.0; (d) Q120-Su1.5; (e) C80-Su1.5; and (f) C106-Su1.5.

the larger urea balls and not of a lamellar-like structure—at least at this scale length.

Also interesting is the comparison of phase behavior at a moderate magnification. Fig. 4 exhibits eight micrographs, two of fully formed foams, four of quenched samples, and two of the crushed samples. It should be noted that the darker stripes observed in Fig. 4b and d are due to variation in the thickness of the section and not to any change in morphological character. Fig. 4a and b show SSu0.0 and SSu1.5, respectively, and illustrate the typical behavior of slabstock foam samples. Both of those two micrographs reveal a uniform dispersion of the aggregates observed in Fig. 3. It also shows no noticeable differences *at this scale* between samples with and without surfactant. However, Fig. 4c and d show that, at the same magnification, dramatically different behavior can be observed in the quenched

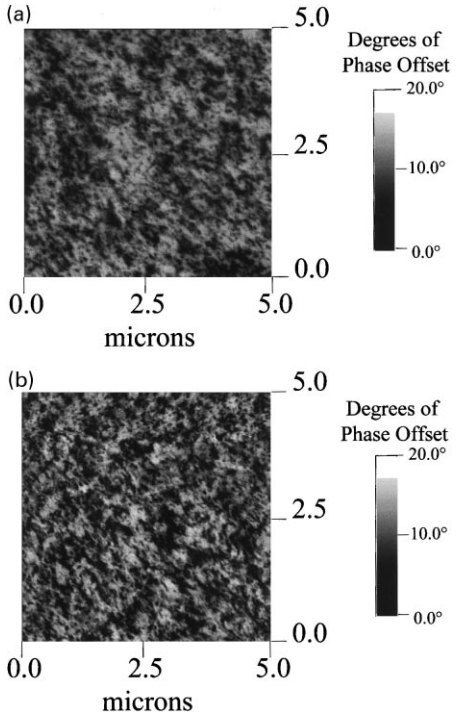

Fig. 6. AFM phase images of two quenched materials: (a) Q100-Su0.0; and (b) Q100-Su1.5. The *z* axis scale has been inverted from the machine default such that higher phase offset is induced by softer material. This is only done in these two images to parallel the TEM micrographs of Figs. 3–5.

samples. Sample Q100-SSu0.0 shown in Fig. 4c reveals large areas with little urea precipitation and other large regions with much aggregation occurring. Sample Q100-SSu1.5 shown in Fig. 4d reveals that this does not occur in foams with surfactant, providing further evidence that surfactant does have a stabilizing influence on urea precipitates. Fig. 4e shows that sample Q120-Su0.0 has aggregates that are more dispersed. This indicates that the additional 20 s of reaction time provided this sample with more stability in preventing large scale aggregation due to a higher degree of covalent bonding than sample Q100-Su0.0 had. Fig. 4f illustrates that sample Q120-Su1.5 had a similar morphology to sample Q100-Su1.5, indicating that with surfactant present, the time of quench made much less of an impact. It is worth emphasizing that the morphology observed in the micrographs of the quenched materials is not supposed to characterize the morphology of the high temperature reactive state. Rather, they characterize the aggregation behavior of the hard segments at that level of covalent cross-linking, concentration of surfactant, and with or without the presence of the cellular structure.

The most intriguing parts of Fig. 4 are in Fig. 4g and h. These two micrographs are of the two foams that were mechanically crushed. Fig. 4g shows that in sample C80-Su1.5 the same morphology was developed as in sample Q100-Su0.0. This indicates that surfactant alone is not enough to prevent large-scale aggregation from occurring. Observing that sample C106-Su1.5 does not exhibit this aggregation but does exhibit a dispersed morphology indicates that being in the collapsed state at the time of urea precipitation plays a large role in the final morphology of the polymer.

Fig. 5 seeks to examine this better by presenting six micrographs of the quenched and crushed samples at the lowest level of magnification used. Fig. 5a shows that the large scale aggregation behavior of sample Q100-Su0.0 was characteristic of the entire polymer sample. It also shows that these aggregates cover spaces of several microns. This is dramatically different than the even distribution seen in Fig. 5b, d or f (samples Q100-Su1.5, Q120-Su1.5, and C106-Su1.5, respectively). Fig. 5c reveals that in sample Q120-Su0.0, although the precipitates are more disperse than sample Q100-Su0.0, some large aggregation can still be seen. Finally, in Fig. 5e it is observed that sample C80-Su1.5 does have a very similar morphology to sample Q100-Su0.0, and that this morphology is characteristic of the whole. Before making final conclusions about the TEM data, two AFM phase images are also presented in Fig. 6a and b to attest to the validity of that technique for use in foam research. Fig. 6a (Q100-Su0.0) and Fig. 6b (Q100-Su1.5) are shown in similar scale for easy comparison to TEM micrographs of Fig. 4c and d. *Also, the scales of the AFM phase images in Fig. 6 have been inverted so that the harder material has lower offset and appears darker just as the urea-rich regions appear dark in the TEM. This was done only to these two images in order to parallel the TEM images for convenience; however, in the rest of this paper all AFM phase images will use the normal scale for the instrument wherein higher phase offset indicates harder material and appears whiter.*

Altogether, the TEM micrographs presented show an interesting pattern. They reveal that when the reactive mixture is allowed to go to completion at high temperature (ca. 140°C), an evenly dispersed morphology is achieved over the whole range of surfactant concentrations studied. Without the stabilizing effect of the surfactant, however, aggregation does occur when quenched prior to reaction completion. Comparison of Figs. 4c and e or 5a and c also shows that allowing the reaction to proceed an additional 20 s stabilizes the urea further so that the precipitates of sample Q120-Su0.0 are smaller. This is attributed to further completion of the gelation reaction. With surfactant this behavior is not observed, and the precipitates are observed to be dispersed regardless of the progress of the reactions. This is taken as direct evidence of the ability of surfactant to influence urea precipitation; however, the mechanism of that influence needs further elucidation. This is why samples C80-Su1.5 and C106-Su1.5 are so important. *These show that the observed behavior is not strictly a direct function of the surfactant but also of the presence of the cellular morphology*. All three samples shown in Fig. 5 that exhibit large-scale aggregation behavior were in the collapsed state when the urea precipitated. All three samples of Fig. 5 that

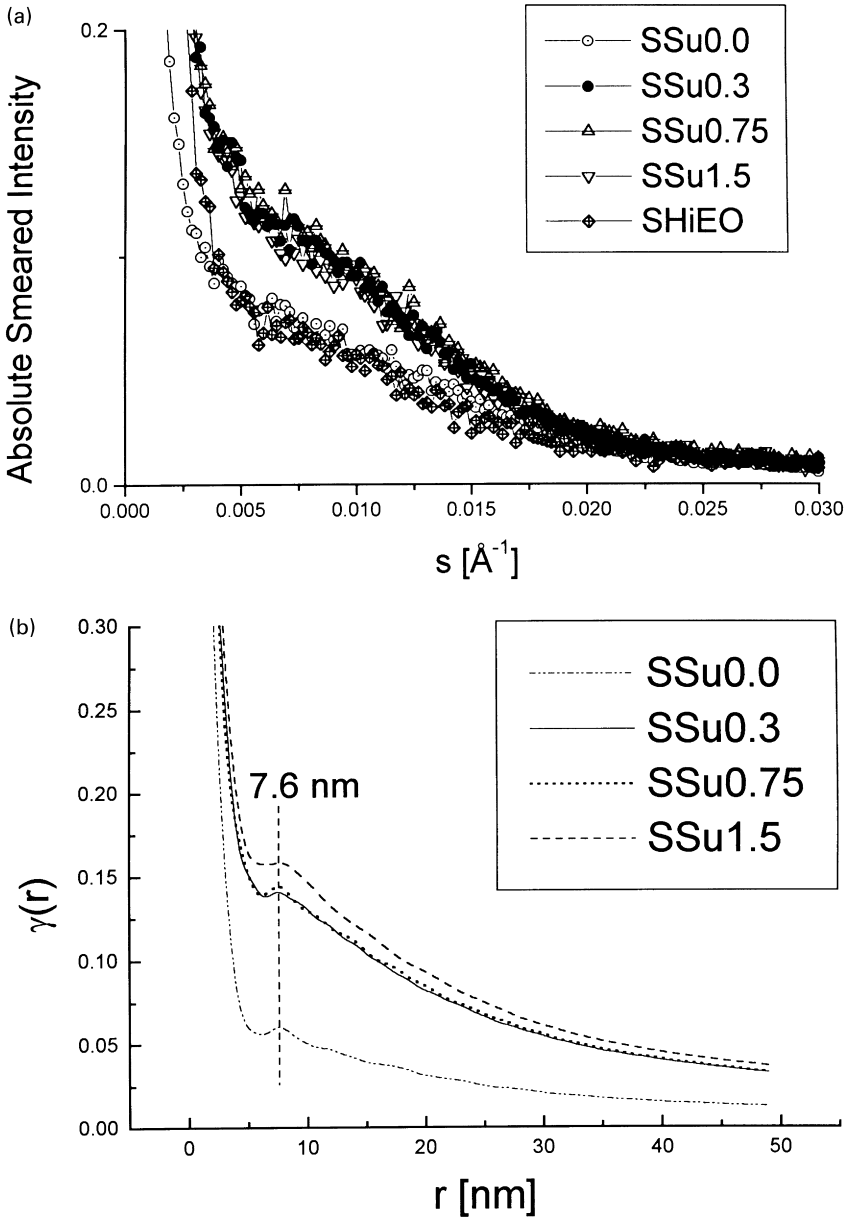

Fig. 7. (a) Small angle X-ray scattering data for foams of varying composition; (b) 3D correlation functions for four slabstock foams of varying surfactant concentration; (c) small angle X-ray scattering data for two foams quenched from reaction at different times; (d) 3D correlation functions for four quenched foams of varying surfactant concentration; (e) 3D correlation functions for two crushed foams of 1.5 surfactant pphp concentration; (f) comparison of the mean chord lengths for all the samples.

show a dispersed morphology still had a cellular morphology at the point of urea precipitation. Why then is there not large-scale aggregation observed in the micrographs of SSu0.0 (Fig. 4a)? It is recalled that sample SSu0.0 is the only sample that collapsed which had a thermal history more similar to a normal foam despite losing some heat in the expulsion of gas upon collapse. This indicates the importance of maintaining a high temperature until the gelation reaction adds enough stability to the system to prevent large-scale aggregation from being induced by dramatic cooling. Such cooling may occur either by quench or by squeezing into a thin film between two unheated metal plates. It can be said from all these micrographs that, without cellular structure, high temperature is necessary to maintain the dispersion of urea precipitate; however, with cellular structure at the point of urea precipitation, thermal history is less important to the phase separation behavior at these scales. This raises the question of what influence does quenching or cooling or spontaneously collapsing have on even lower scale morphology, and this will be examined next.

SAXS has been widely used in polyurethane foam research [28] to follow phase separation behavior; however, the laws of scattering and the wavelengths of X-rays only

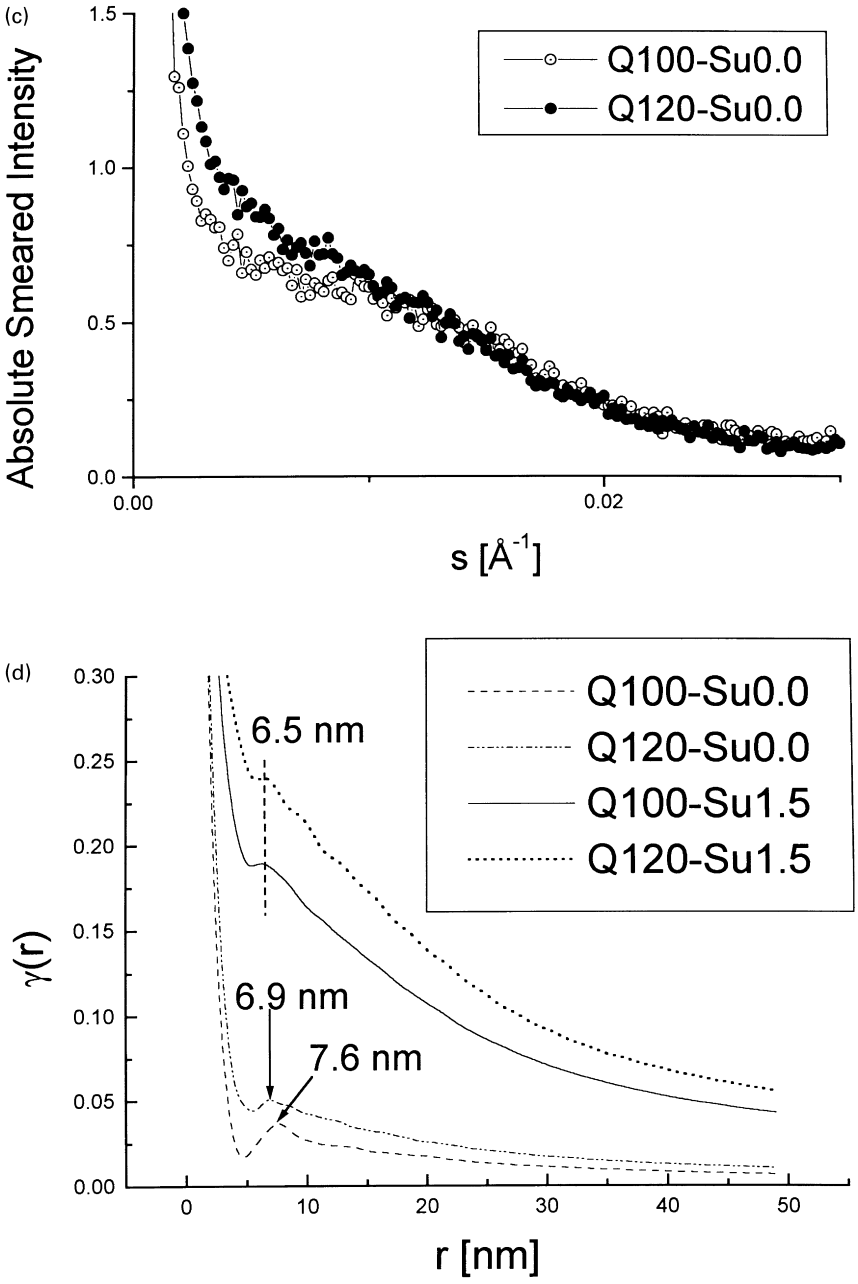

Fig. 7. (*continued*)

allow this technique to examine scales smaller than what is needed here for a complete analysis of phase behavior. This technique thus explores phase separation behavior on length scales between TEM and WAXS. Fig. 7a–e show some representative SAXS data and the results of the correlation function analyses. One thing that this reveals is that all of the foams, including SHiEO, are microphase separated. It can also be observed in Fig. 7a that the scattering intensity of SSu0.0 is much lower than that of the other completely reacted samples. This is suggestive of less microphase separation in the collapsed material. Taking the Fourier transform of the scattering curves in the proper manner [29] can lead to the three-dimensional (3D) correlation functions shown in Fig. 7b. This is essentially a plot of the probability that a rod of length *r* has both of its ends in a domain of similar electron density [29]. Fig. 7b clearly shows that every completely reacted foam exhibits an interdomain spacing of 7.6 nm. Thus revealing that the surfactant concentration does not have a detectable influence on the interdomain spacing of the completely reacted foams.

However, Fig. 7c shows the SAXS data for Q100-Su0.0 and Q120-Su0.0 wherein it can be seen that the patterns are clearly different although a definite shoulder position is difficult to place. Fig. 7d shows the 3D correlation functions for all of the quenched materials, where it can be seen that the foams with surfactant appear to have nearly identical

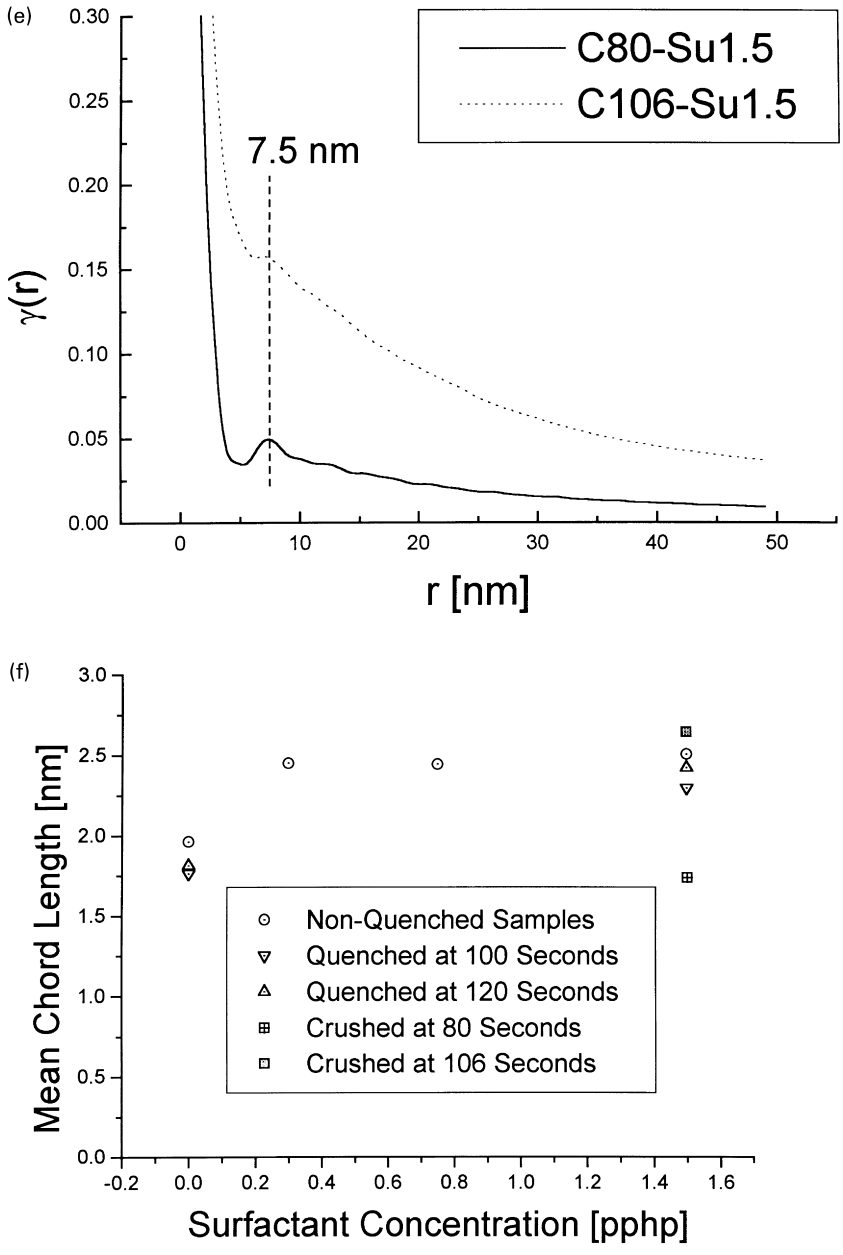

Fig. 7. (*continued*)

distributions, both having most probable interdomain distances of 6.5 nm. Without surfactant, however, quenching at 100 s changes the microphase separation behavior significantly, developing an interdomain spacing of 7.6 nm. It is observed that the Q120-Su0.0, which had an additional 20 s in the high temperature reactive state, has a spacing of 6.9 nm, seeming to approach the spacing of the surfactant-containing quenched materials. It is also noted that in Fig. 7e the crushed materials are seen to both have interdomain distances of 7.5 nm. This confirms what is observed in the TEM data: adding reaction time alters the phase separation behavior of these foams.

These results indicate that the most probable interdomain distance as revealed by SAXS is not strongly influenced by changes in surfactant concentration. However, another parameter that can be obtained from SAXS, the mean chord length, does exhibit some systematic changes. This parameter is interpreted to be the average size of the hard domains throughout the sample [29]. This interpretation applies to dispersed components, and it is strongly dependent on the shape of each phase in the system [29]. For more lamellar-like or sponge-like structures, the mean chord length or inhomogeneity length characterizes the harmonic average of the chord lengths in each phase [29]. The results of this analysis performed on each sample are shown in Fig. 7f. The clearest thing observed is the subtle yet consistent increase in the mean chord length of the non-quenched samples as the surfactant increases. It appears from Fig. 7f

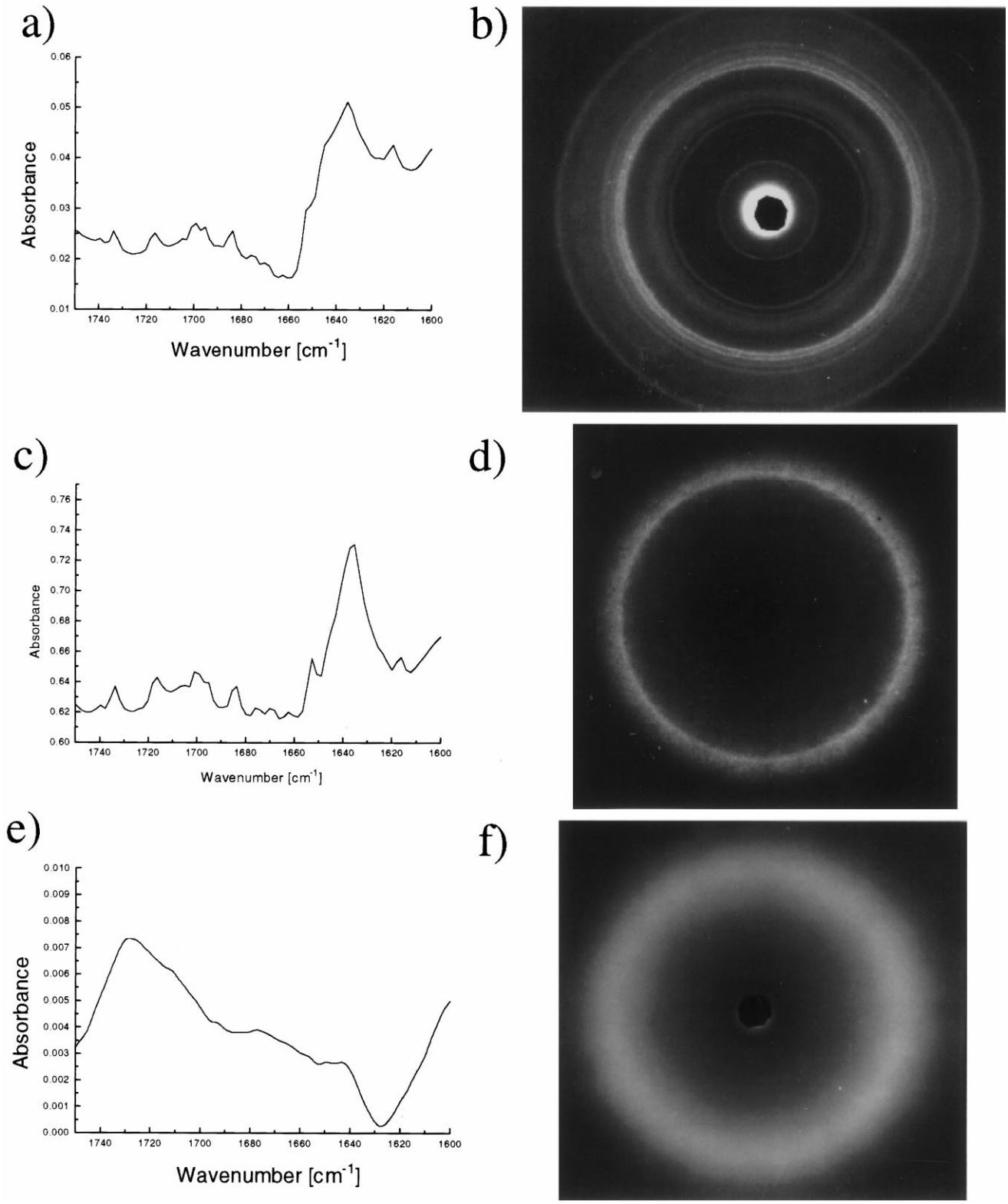

Fig. 8. Correlation of Fourier transform infrared spectroscopy and wide-angle X-ray scattering for polyurethane foams: (a) transmission mode FTIR spectrum of PUA; (b) WAXS pattern of PUA; (c) transmission mode FTIR spectrum of PUSu; (d) WAXS pattern of PUSu; (e) attentuated total reflectance mode FTIR spectrum of ShiEO; (f) WAXS pattern of ShiEO.

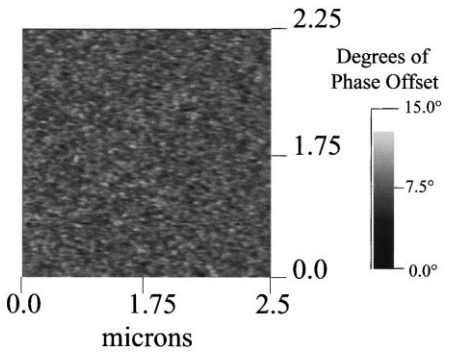

Fig. 9. AFM phase image of SHiEO.

that the mean chord length step jumps with the first increment of surfactant added and is fairly stable after that, varying only slightly (increasing from 1.96 nm in SSu0.0 to 2.50 nm in SSu0.3 to 2.51 nm in SSu1.5). This is significant since SSu0.3 had the lowest surfactant concentration of any sample which maintained a cellular structure. So it appears from Fig. 7f that a mean chord length of ca. 2 nm may be expected in collapsed materials, and a length of ca. 2.5 nm may be expected in materials that have a cellular structure.

Another systematic trend is that the chord length increases steadily the longer the foam is left at the high temperature reactive condition. For instance, the 0.0 surfactant pphp samples exhibit a 1.76 nm chord length when quenched at 100 s, 1.81 nm if quenched at 120 s, and exhibit a chord length of 1.96 nm if not quenched at all. By comparing samples quenched at the same time, it also can be observed that in every case the sample with surfactant exhibits a longer chord length. For example, Q100-Su0.0 has a chord length of 1.76 nm whereas sample Q100-Su1.5 is spaced at 2.30 nm. This reveals a new pattern not observed in TEM: the presence of surfactant seems to facilitate either the growth of the hard segments themselves or the phase separation process as the hard domains become larger.

These results show progressing structural development in terms of increasing mean chord length with increasing time until quenched or crushed. It is not surprising that a foam quenched from the reaction to liquid nitrogen temperatures would not achieve the same domain sizes that a fully developed foam has. However, it is especially interesting that a sample that was crushed and not quenched, C80-Su1.5, has a lower mean chord length (1.74 nm) than either C106-Su1.5 (2.64 nm) or SSu1.5 (2.51 nm). This indicates that being in the collapsed state prior to urea precipitation apparently does alter the microphase morphology of the foams. While this is additional evidence that the surfactant does not play a direct role in the development of hard domain structure, it *does further suggest that development of cellular structure has a strong influence on that process*.

These results have shown that the lack of large surface area of a gas–liquid interface at the time of urea precipitation has a significant influence on solid state morphology in crushed and quenched materials. However, if high temperature is maintained in the collapsed state (as shown in the micrographs of SSu0.0) only a subtle change in micron-scale morphology is observed. These two apparently disparate results may indicate that, at the molecular level, a lack of surfactant has had an effect. Such an effect may only become readily observable at microscopic levels after the system is kinetically jarred by something like a quench in liquid nitrogen or by being mechanically crushed between two room temperature metal plates. If a molecular level effect does indeed exist, it should be detectable by FTIR, WAXS, and AFM.

The FTIR technique has been well established as a method for evaluating the level of hard segment hydrogen bonding in these materials. Although the WAXS studies on slabstock foams show that they are clearly not semi-crystalline materials, it has been widely observed that a distinct scattering or diffraction peak occurs in the patterns corresponding to ca. 4.7 Å spacing [1,2]. This peak has been widely attributed to ordering within the urea based hard domains or aggregates without full knowledge of the exact source of its reflection. Fig. 8a–f show the correlation that exists between WAXS and FTIR for samples UPA, UPSu, and SHiEO. It can be observed that in Fig. 8b, sample UPA, which is a pure polyurea powder based on TDI 80, has the many reflections expected of the highly crystalline powder. These reflections have been reported by other workers [2], and it is particularly noted that the strongest reflection is a doublet peak occurring at ca. 4.7 Å. The FTIR spectrum shown in Fig. 8a reveals many absorbances, but one of particular strength occurs ca. 1640 cm^{-1}, corresponding to the bidentate hydrogen bonding of the urea carbonyl group. Fig. 8c shows that the FTIR of sample UPSu still exhibits a strong ca. 1640 cm^{-1} peak, indicating that the surfactant has not altered the bidentate hydrogen bonding of the urea. The WAXS pattern of UPSu, however, shows that, even with only the surfactant present, the only remaining periodic spacing in the sample is that which corresponds to the 4.7 Å ordering. This clearly indicates that not only does surfactant influence the way urea rich hard segments pack together, it only leaves one type of ordering at all, the 4.7 Å spacing. Comparison of these figures thus give strong evidence that the 4.7 Å spacing arises from the bidentate hydrogen bonding between urea linkages within the hard domains.

Final evidence of this attribution is given by sample SHiEO in Fig. 8e and f. In the FTIR spectra of this high ethylene oxide content foam, it is observed that the bidentate hydrogen bonding is highly disrupted or decreased relative to the free urea peak at 1710 cm^{-1}. Fig. 9 shows an AFM phase image of SHiEO to confirm along with the SAXS data that SHiEO does have a two-phase morphology; however, as the FTIR shows the hard domains have nearly no internal ordering within them. Therefore, as it is observed in the corresponding WAXS pattern that the 4.7 Å reflection is dissipated and only a diffuse amorphous halo remains, it becomes apparent that observing the WAXS

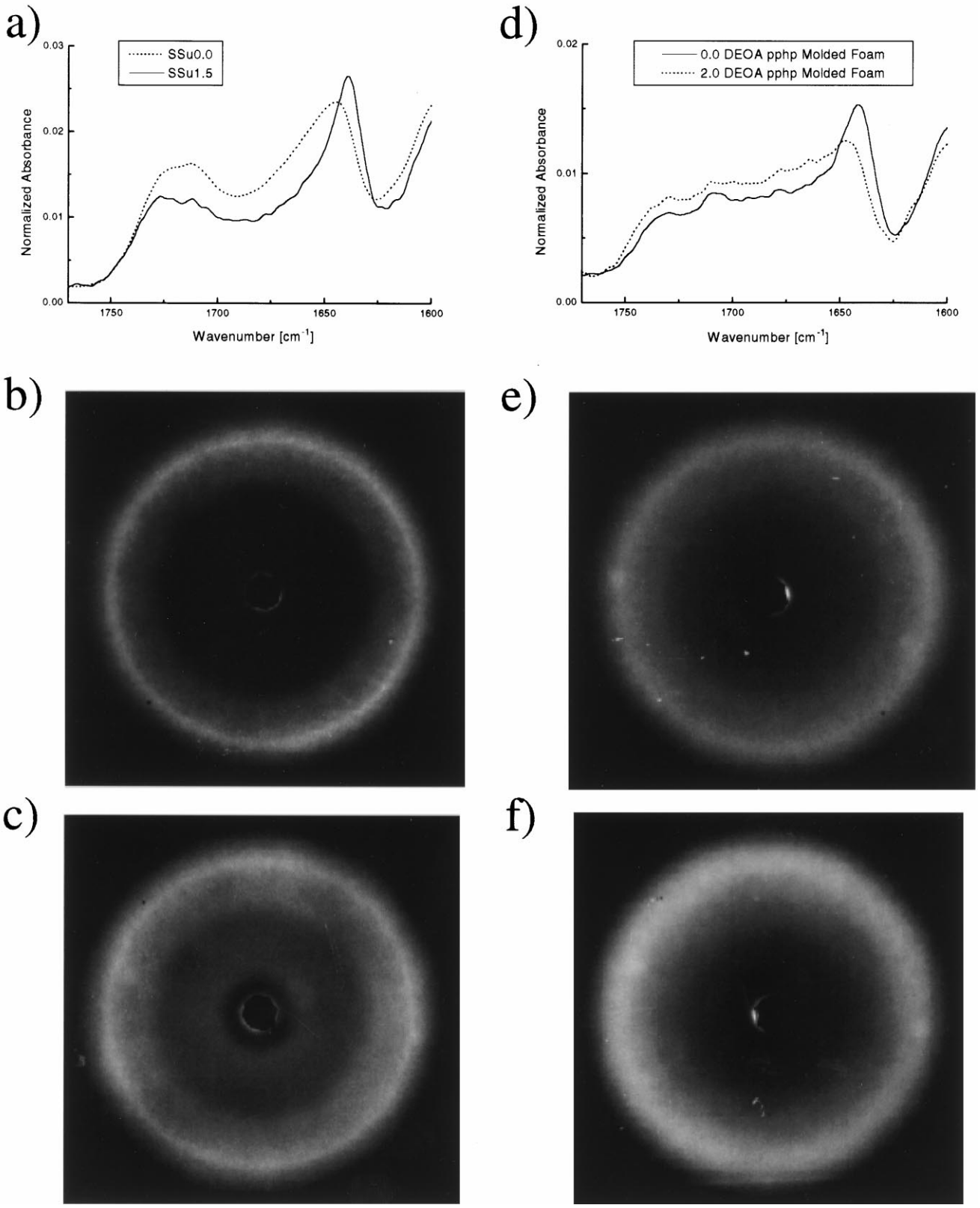

Fig. 10. Fourier transform infrared spectroscopy and wide-angle X-ray scattering of polyurethane foams: (a) attentuated total reflectance mode FTIR spectrum of SSu0.0 and SSu1.5; (b) WAXS pattern of SSu1.5; (c) WAXS pattern of SSu0.0; (d) attentuated total reflectance mode FTIR spectrum of MD0.0 and MD2.0; (10e) WAXS pattern of MD0.0; and (f) WAXS pattern of MD2.0.

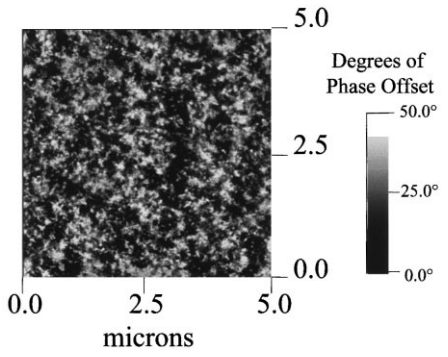

Fig. 11. AFM phase image of SSu1.5, representative of a typical image from the polyurethane foams in this study.

peak is a way of confirming that the bidentate hydrogen bonding is present in the system and that the hard segments are well ordered.

The above knowledge is applied to the study of surfactants in Fig. 10. As Fig. 10a shows, removing all surfactant has a dramatic influence on the shape of the FTIR spectra in the carbonyl region. Three main differences are observed. Two of these are that the level of bidentate hydrogen bonding has decreased (the absorbance ca. 1640 cm^{-1}) and the level of free or dissolved urea particles has increased (higher absorbance at 1710 cm^{-1}). The other change is that the hydrogen bonding peak has actually shifted towards 1650 cm^{-1} indicating an increasing degree of monodentate hydrogen bonding. This indicates that the final solid polymer is without some of its strongest physical bonds. It is interesting to note that as shown in Fig. 10b and c, the 4.7 Å reflection is still present in the WAXS. This indicates that within the hard domains themselves, there is still significant bidentate packing present. Therefore, this suggests that the higher level of free urea and monodentate hydrogen bonded urea stems from more urea still being out in the matrix and not fully precipitated.

To clarify this argument, data from two molded flexible polyurethane foams have been added as shown in Table 1. By studying the tan delta peak from DMA, as will be done later for this study, it was shown that these two foams have similar degrees of phase separation or polyol matrix purity [5]. In Fig. 10d it is shown that by adding the crosslinking agent diethanol amine (DEOA), the carbonyl region of the FTIR spectra transforms similarly to that of the no surfactant foam in Fig. 10a: the peak at 1710 cm^{-1} rises, the absorbance at 1640 cm^{-1} falls, and the peak of hydrogen bonding shifts toward 1650 cm^{-1}. However, as can be seen in Fig. 10e and f, the addition of DEOA completely disrupts the 4.7 Å reflection. This is in complete contrast to the effect of removing the surfactant, and it points out the importance of using both of these techniques in studying the hard domains of polyurethane foams. Other studies by the authors [15] has shown that DEOA resides within the hard domains and disrupts the ordering there as observed by WAXS. *Therefore observing hydrogen bonding via FTIR alone is not sufficient to conclude that ordering exists within the hard domains. Likewise observing a 4.7 Å reflection via WAXS indicates bidentate hydrogen bonding and good ordering within the hard domains or urea aggregates, but is not sufficient to conclude that the highest level of phase separation has occurred as shown by FTIR or by the polyol glass transition temperature*. These techniques thus complement one another in discerning the microphase separation behavior of polyurethane foams. The way that DEOA alters the composition of the hard segments precludes good packing in hard domains even in the presence of good phase separation. However, the slabstock foam without surfactant exhibits good hard domain ordering and its FTIR behavior can only be explained as a reduced degree of phase separation.

Another method for examining the phase separation behavior of these systems is with the phase images of AFM. It should be emphasized that, as described in the methodology section, a “phase image” is a two-dimensional (2D) plot of the phase lags or phase offsets recorded by the instrument as the tip interacts with the surface being studied.

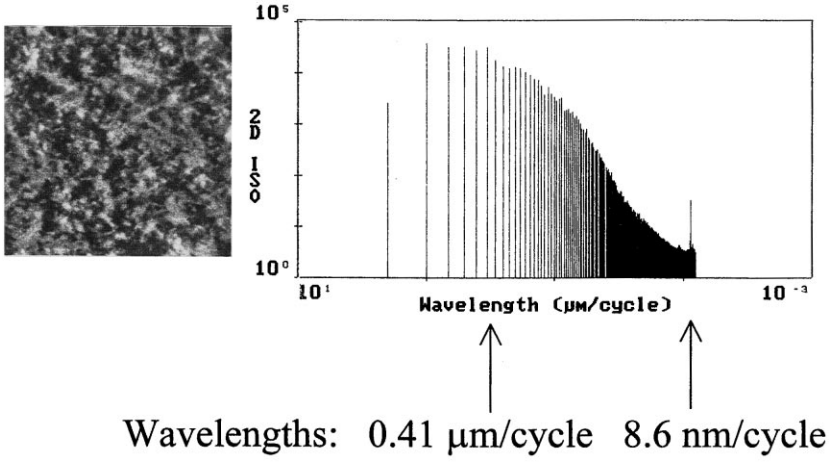

Fig. 12. Power spectral density (Fourier transform analysis) of SSu1.5 illustrating the two scale lengths (ca. 0.5 μm and ca. 8 nm) in the distribution of wavelengths that characterize the distribution of domains with similar phase offsets in the surface.

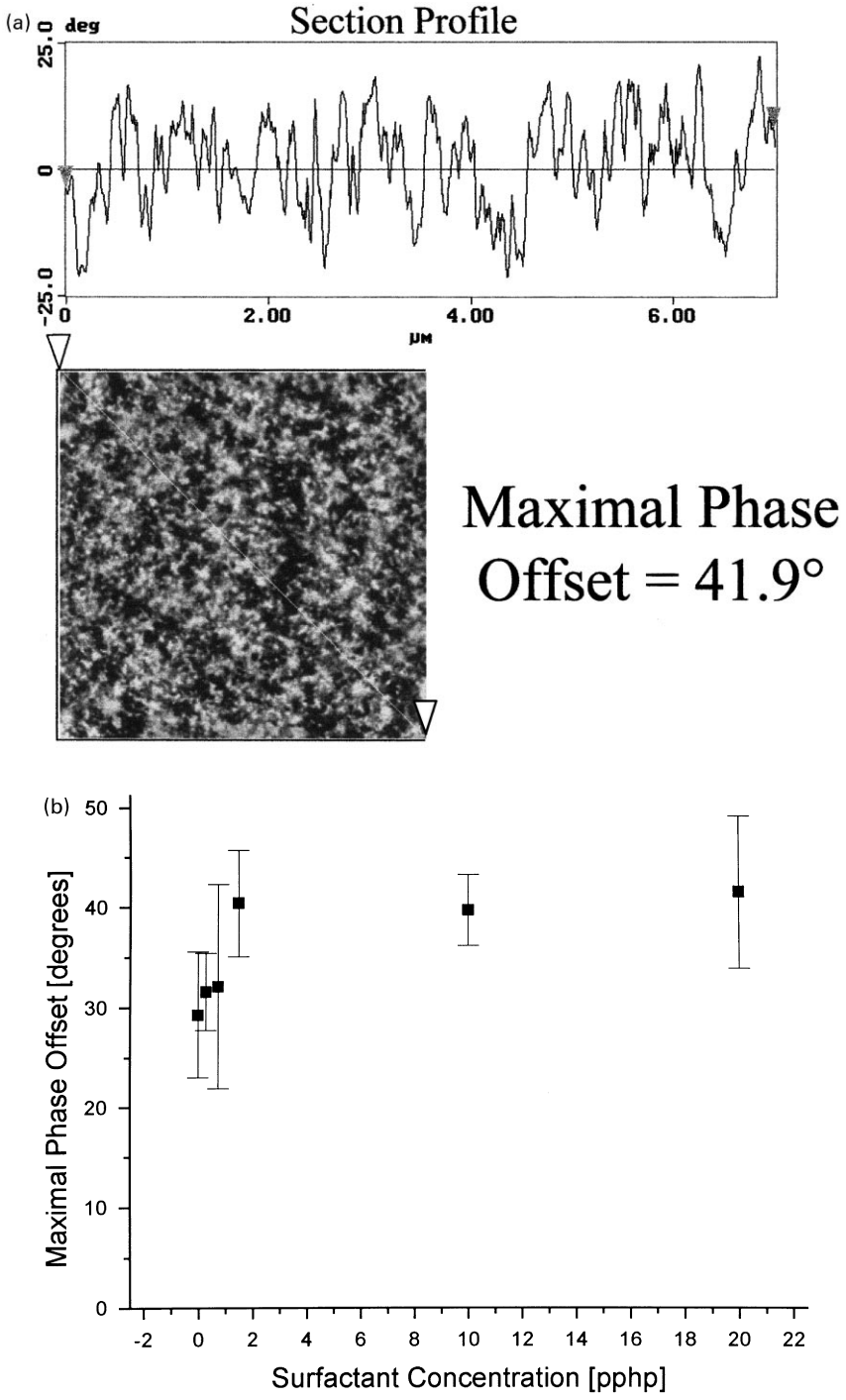

Fig. 13. (a) Representative section analysis of the phase image SSu1.5 shown in Fig. 11; (b) maximal phase offsets for foams of various surfactant concentration; (c) comparitive trends between the 1640 cm^{-1} absorbance from FTIR and the maximal phase offsets of AFM tapping mode; (d) maximal phase offsets for foams in various states (fully developed, quenched, or crushed); (e) 1640 cm^{-1} absorbances from FTIR for foams of various states. This demonstrates that the 1640 cm^{-1} absorbance is consistent for each level of cure but cannot be used to explain the behavior of samples at different states shown in Fig. 13d.

"Height images" are recorded simultaneously but because the surfaces studied here have been cryotomed smooth they are disregarded. Phase images of polymer systems can be used qualitatively to describe morphology, or they may be numerically examined to quantitatively characterize either periodically occurring structure in the surface or levels of phase offset induced by the tip-surface interactions. Fig. 11 shows an AFM phase image of sample SSu1.5 wherein the scale is oriented so that harder material is shown by larger phase offsets. Fig. 12 shows a Fourier transform analysis of

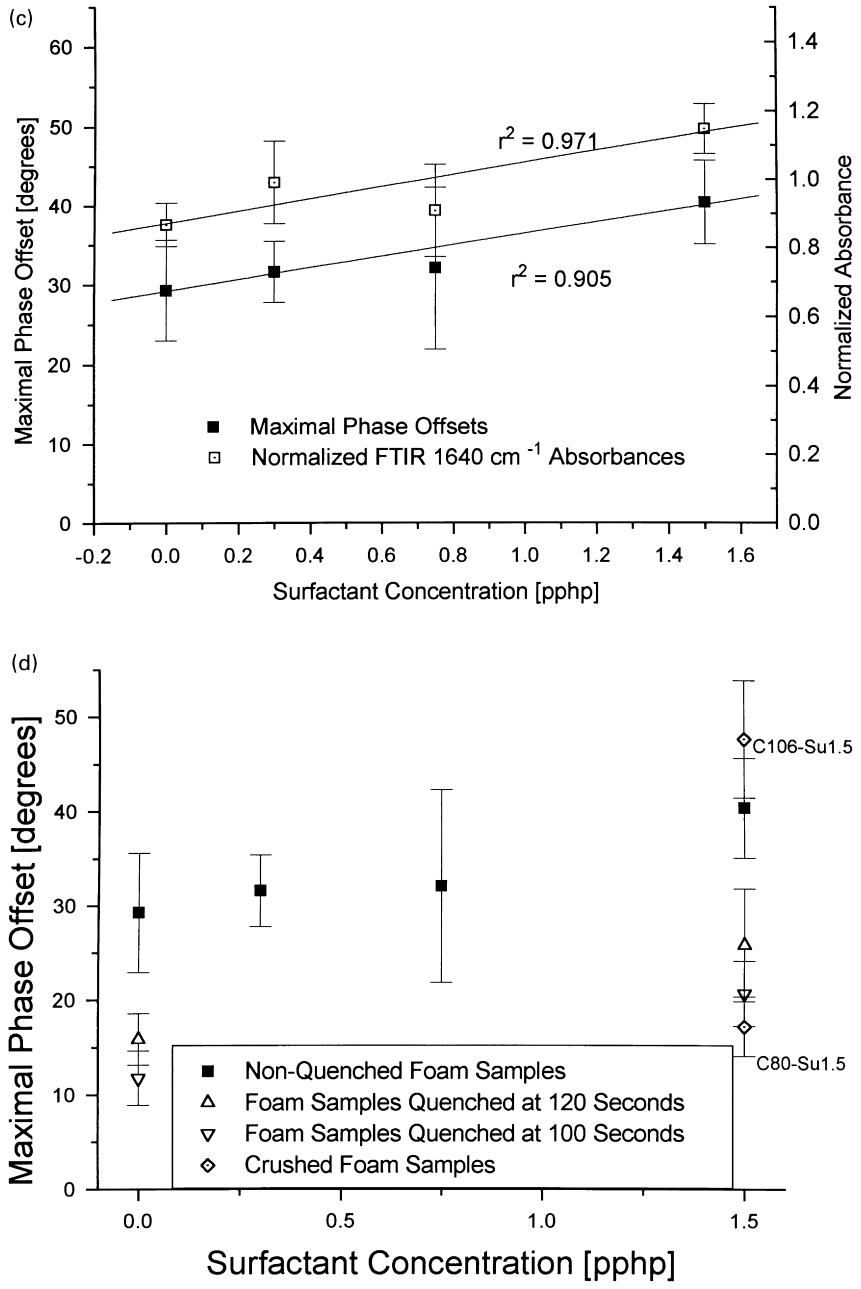

Fig. 13. (*continued*)

the surface of sample SSu1.5 called the power spectral density. The transform utilized and further details of this analysis with examples are available in Ref. [30]. Basically, how often a phase offset occurs can be characterized in terms of a wavelength, and Fig. 12 shows the distributions of the different wavelengths that occur throughout the image. Thus the most often recurring wavelengths are shown as peaks in the distribution and provide a way to find important structural parameters in the surface. It is worth pointing out that every slabstock sample examined with this technique exhibited peaks at two scale lengths in its distribution, a major one at ca. 1.0–0.5 μm and a much smaller one at ca. 8–10 nm. This signals that AFM may provide a systematic way to quantitatively characterize the micron scale aggregation behavior often observed in slabstock systems. Also, the smaller maximum appears to correlate with the interdomain distances typically observed in these materials via SAXS. A similar correspondence between SAXS and AFM was recently reported in other materials by McLean and Sauer [26]. For flexible polyurethane foams this suggests that AFM is probing the scale lengths of the hard domains; therefore, following phase offsets may be a way to characterize and detect alterations in the mechanical properties of the hard domains themselves.

Evaluation of the relative hardness of the urea-rich

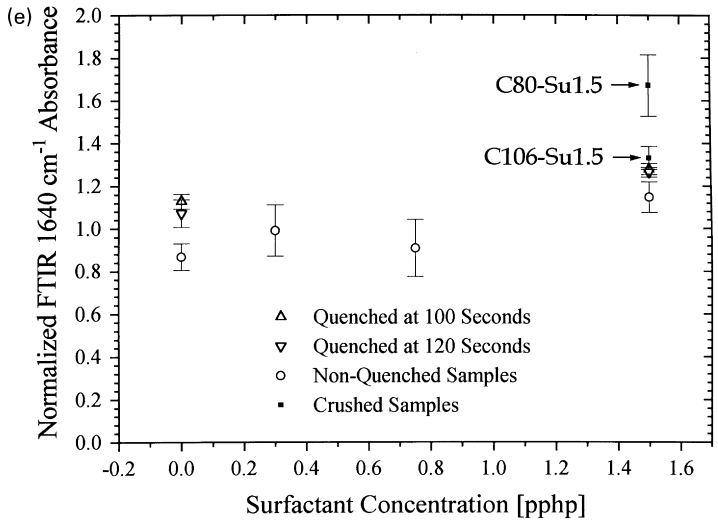

Fig. 13. (*continued*)

regions was accomplished by averaging the maximal phase offsets from several scans for every sample. Fig. 13a shows a section analysis for the phase image of Fig. 11, which shows how the hardness varies along a line drawn across the inserted figure. This provides a way to measure the maximal phase offset at many places on the surface. For the SSu series, as shown in Fig. 13b, above surfactant concentrations of 1.5 pphp, the average relative hardness does not increase. This indicates that the surfactant helps the urea precipitates to achieve their hardest state, but the surfactant does not itself add hardness. Below 1.5 pphp, this relative hardness is seen to be dropping off with decreasing surfactant concentration. This region is examined in more detail in Fig. 13c. Here it is observed that the increasing maximal phase offset matches the earlier trend of increasing the 1640 cm^{-1} normalized peak FTIR absorbance. This matches the increasing relative hardness to increasing the content of the strongest type of hydrogen bonding. It is also noted that the outlier from the trend of increasing the 1640 cm^{-1} absorbance, foam SSu0.75, is also an outlier from the trend of increasing phase offset. That helps to confirm the correlation between the two techniques that ordering in the hard domains or urea aggregates relates directly to their hardness which leads to the higher phase offset observed on the AFM. Finally, in Fig. 13d, the results of the collapsed and quenched samples are added. Here it is seen that the same increase in relative hardness with surfactant addition is observed in the quenched samples. It is also noted that the additional 20 s of reaction time increases the relative hardness towards that of the completely reacted foams. It is also noted that the foam which was mechanically compressed at 80 s has lower offset than the same surfactant level quenched at 100 s. Further, it is observed that the foam crushed after urea precipitation has a relative domain hardness near the same level as that of the final foam.

It is important to point out that the level of bidentate hydrogen bonding alone as shown by FTIR cannot completely explain the trends of maximal phase offsets. This is shown in Fig. 13e. Within a given state (e.g. non-quenched, quenched, or crushed) increasing amounts of bidentate hydrogen bonding are observed as surfactant concentration increases. However, comparisons across the various states show opposite trends to those observed in Fig. 13d. Q120-Su0.0 has more bidentate hydrogen bonding than SSu0.0, and Q100-Su0.0 has more than Q120-Su0.0. This demonstrates that while the increasing relative hardness shown by AFM is related to bidentate hydrogen bonding, these physical bonds cannot completely explain the behavior. Based on Fig. 7f, it is thus hypothesized that the increased size (i.e. mean chord lengths) of the hard domains in addition to their increased level of hydrogen bonding leads to what is observed via AFM as higher relative hardness.

These AFM results are consistent with themselves and are also well aligned with the data from the other structural analysis methods. Together, they indicate that the surfactant level has an effect on the development of the foam morphology at every level. Further evidence of this comes from thermal analysis via DSC and DMA. Fig. 14a shows the tan delta plot from DMA. This shows that without surfactant, the polyol has a distinctly higher T_g, indicating much more dissolved polyurea in the polyol. With surfactant, however, the glass transition occurs a few degrees lower, indicating a purer polyol and better phase separation. This is also shown in that the tan delta peak height of SSu0.0 is significantly higher than the other peaks, which indicates that more “stiff” hard segment material is distributed throughout the polyol matrix [19]. Further, as shown in Fig. 14b, both quenching and mechanical crushing disrupts the process of phase separation. This is also exhibited in Fig. 14c. These figures show that surfactant concentration does not directly control the degree of phase separation. The rise in the tan delta peak heights in moving from 100 to 120 s of quench shows that quenching the foam freezes some of the

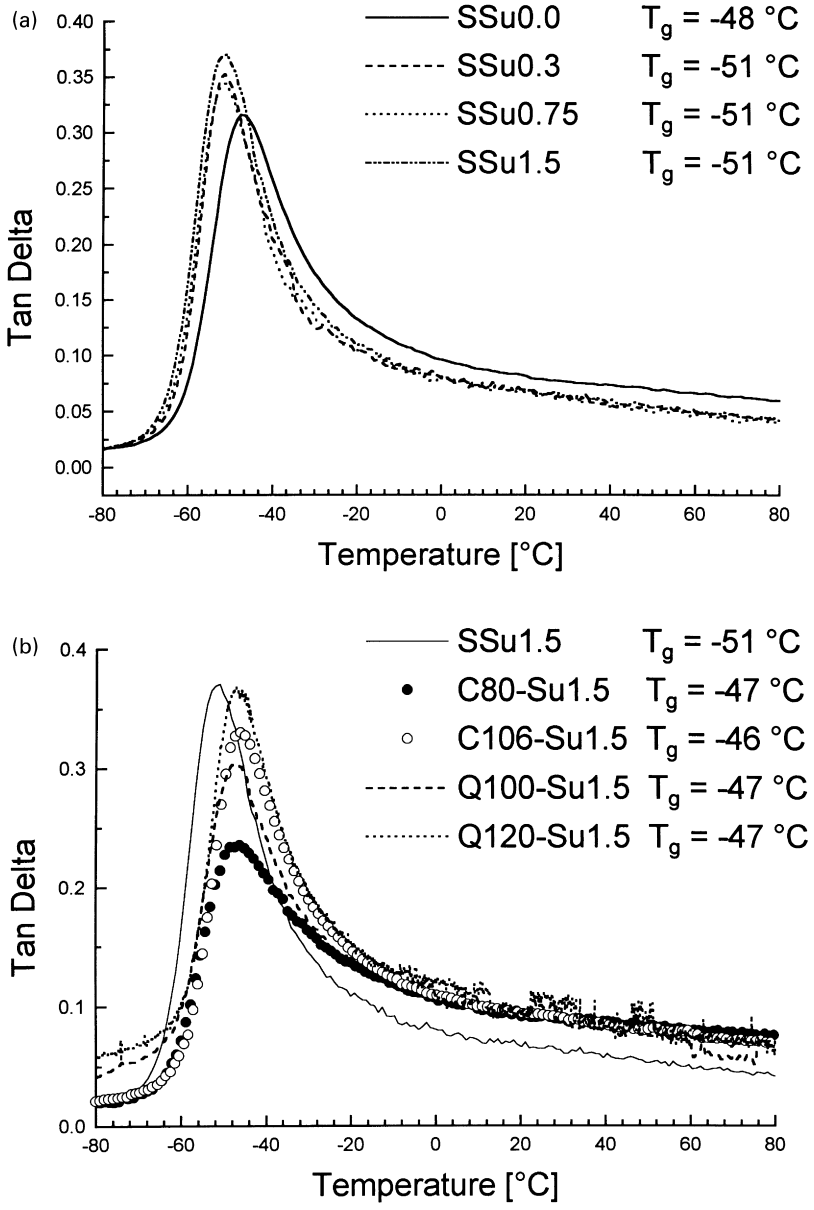

Fig. 14. Tan delta from DMS for: (a) samples of various surfactant concentrations; (b) samples with 1.5 surfactant pphp concentration at different states; (c) all samples that collapsed spontaneously, were quenched, or were crushed.

polyurea out in the polyol matrix and prevents less complete phase separation. These figures also show that mechanical collapse or spontaneous collapse has similar effects. These trends were confirmed by DSC, but that data is not presented here. This important data further indicates that the process of bubble growth or the presence of large gas–liquid interfacial area may well play an important role in the process of phase separation.

The tanδ behavior of these systems points out that for these flexible polyurethane foam systems, a difference in the location of the tan delta peak may not necessarily mean as much as the relative peak height. Every foam that was quenched or that collapsed has the same peak location has shown in Fig. 14c. Even C106-Su1.5 has a glass transition at −46°C which is significantly higher than that of SSu1.5 (−51°C). This indicates that remaining at the high temperature of the reactive state (ca. 140°C) throughout the curing of the material while still in the presence of the cellular structure are important to the precipitation of the polyurea. The data also shows that comparing the relative heights of the tan delta peak may be a more effective way of evaluating mobility in the polyol phase. It is also worth pointing out that it is not assumed that the polyol is completely free of dissolved hard segments even in SSu1.5; as it is known that some low molecular weight hard segment material does form, some of that is probably still dissolved in the matrix. Thus a higher glass transition indicates a lower polyol purity relative to that which is achieved by the fully cured slabstock systems.

This study has so far shown that surfactant concentration

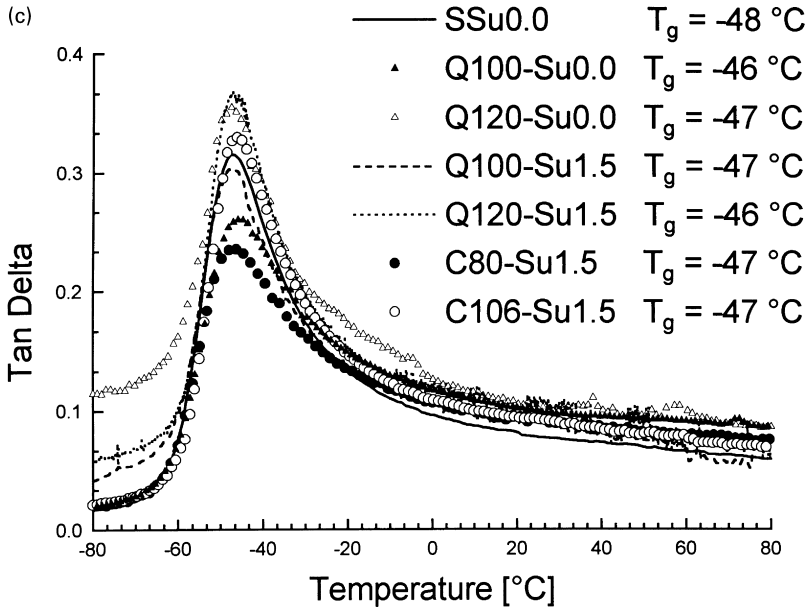

Fig. 14. (*continued*)

has an influence on the degree of phase separation and phase ordering in the foams. This is thought to occur as a secondary effect. The presence of the surfactant primarily stabilizes gas bubbles and the nascent cellular structure, thus incorporating a large surface area of the high energy liquid–gas interface throughout the reactive mixture.

The secondary effect may arise from some combination of two sources. One source may be a preferential ordering at the interface of one component in the reactive mixture. The importance of that ordering would become of greater significance as the windows grow thinner, gaining surface area and losing material between interfaces. This ordering at the interface might thus enhance the process of phase separation during bubble growth. A corollary to this would simply be the presence of that large interfacial area at the time of urea precipitation. As the hard domains begin to organize, having the interface present may promote phase separation and the dispersion of the hard domains. It is known from other systems that amphiphilic particles form at oil/water interfaces, so a mechanism for this behavior suggests itself. If the surfactant molecules prefer to arrange themselves on the gas/liquid interface, their polyether block could, through hydrogen bonding, associate with the developing hard segments. These anisotropic particles might then serve as seeds for further polyurea precipitation. When that interface is unavailable (as in C80-Su1.5), surfactant molecules may associate into micelles in the fluid, inducing aggregation at their surfaces. Thus, without the presence of the gas/liquid interface, it is possible that the urea balls aggregate to sizes at which associations between them can occur, leading to the similarities in storage moduli for samples like SSu0.0 and C80-Su1.5 in Fig. 15c. This might explain how the aggregation behavior observed in Fig. 2 relates to the properties observed in the DMA.

A second source may be that the growth process of the bubbles in the mixture induces flow from the lamellae between bubbles (soon to be windows) into the plateau borders (becoming cell struts). The mixing that would occur during the draining fluid flow might assist in promoting the organization of hard domains or urea aggregates. Given the high viscosity of the liquid at this point in the gelation reaction, it is not suggested that the kind of mixing due to turbulent flow occurs at this point. However, the laminar flow that probably occurs would allow the polyurea in each layer further away from the gas–liquid interface to aggregate to developing precipitates. Without this additional flow, molecular diffusion may be too slow to allow the precipitates to completely form and it may slow the progress of the gelation reaction. This second hypothesis would explain the urea aggregation behavior observed earlier in Figs. 4c, g, 5a, c, and e.

DMA also provides a look at the stiffness behavior of these foams. By normalizing the storage modulus to 3×10^9 Pa in the glassy region, the density variations between samples due to cellular structure are removed [14,19]. The results of this are shown in Fig. 15a, and it is seen that, without surfactant and without internal urea domain ordering, sample SSu0.0 has a much broader glass transition and a softer modulus in the rubbery region. These two observations support the hypothesis that lack of surfactant ultimately results in more dissolved urea and less internal organization within the hard domains. Fig. 15b shows the storage moduli for all materials at 1.5 surfactant pphp. This shows that the crushed materials have very similar properties to the SSu0.0 material, indicating again the importance of maintaining a cellular structure to properties. This is further demonstrated by the quenched materials in that figure that show similar behavior to SSu1.5. Recalling that

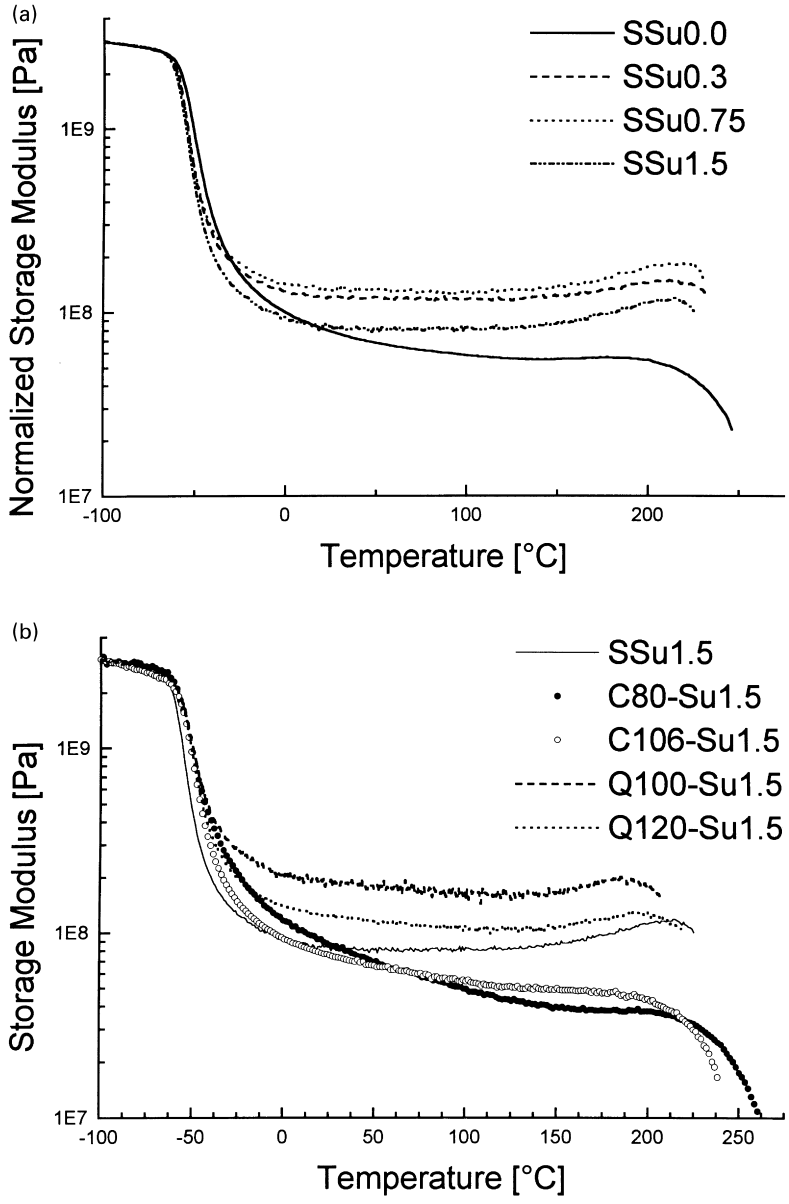

Fig. 15. Storage modulus from DMS for: (a) samples of various surfactant concentrations; (b) samples with 1.5 surfactant pphp concentration at different states; (c) all samples that collapsed spontaneously, were quenched, or were crushed.

these foams were quenched in liquid nitrogen and then allowed to warm to room temperature, that is, they pass through the glass transition of the polyol, it is concluded that precipitation of the existing urea groups occurred in the presence of a cellular morphology. Bringing even more confirmation to this is Fig. 15c, which shows that all of the materials which collapsed have similar properties in showing softer rubbery moduli and broader glass transitions than any material that maintained a cellular structure.

5. Conclusions

This study has shown that surfactant concentration has an influence on the degree of phase separation and hard domain ordering in flexible polyurethane foams. This is thought to occur as a secondary effect, where the presence of the surfactant primarily stabilizes gas bubbles and the cellular structure during the urea precipitation. The secondary effect is suggested to be a combination of ordering at the gas–liquid interface and the influence of increased mixing due to cell growth, leading to the observed higher degrees of phase separation and higher concentrations of hard domains organized via hydrogen bonding. These conclusions apply to foam and collapsed materials, which experience typical thermal histories. Without the presence of the cellular structure at the time of urea precipitation, foams both with and without surfactant were observed to develop large urea

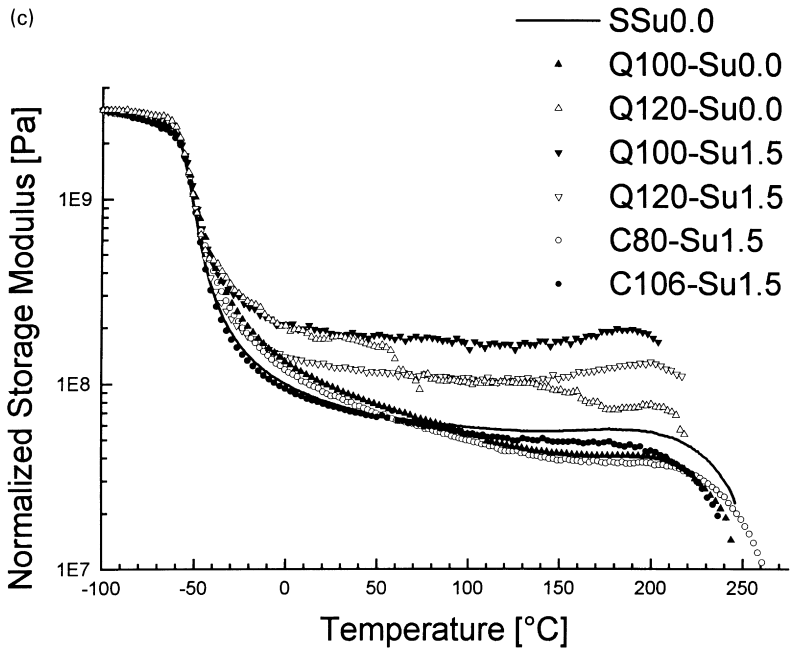

Fig. 15. (*continued*)

aggregations. These exhibited no well-defined structure via TEM, indicating that what connectivity exists may occur as associations between polyurea aggregates. The nature of those associations would be highly dependent on the geometry of the aggregations, whether more spherical or lamellar-like. The possibility of varying thermal history in collapsed materials to achieve properties similar to the foams is a focal point of current work.

This work has not only illustrated the importance of organization within hard domains, but has also brought together many different techniques in probing that organization. A high ethylene oxide content foam was used to show that phase separation, as shown by SAXS, does not imply urea precipitation as shown by either FTIR or WAXS. Further, that high ethylene oxide content foam and two series of urea powders were used to document that the 4.7 Å WAXS reflection widely observed in polyurethane foams correlates to bidentate hydrogen bonded urea groups. AFM was also shown to be a valuable and quantitative tool for probing both phase separation morphology and relative urea domain hardness.

Acknowledgements

This work has been financially supported by Goldschmidt AG and their support is gratefully acknowledged. We also thank Helmut Schator for directing the slabstock foaming experiments at Goldschmidt AG. Molded foam samples were supplied by the Dow Chemical Company, and their generosity is greatly appreciated.

References

[1] Herrington R, Hock K. Flexible polyurethane foams. 2nd ed. Midland, MI: Dow Chemical Co, 1997.
[2] Lidy WA, Rightor E, Phan Thanh H, Cadolle D. Proceedings of the Polyurethanes Expo 96. SPI Polyurethanes Div, 1996, p. 119.
[3] Armistead JP, Wilkes GL, Turner RB. J Appl Polym Sci 1988;35:601.
[4] Dounis DV, Wilkes GL. Proceedings of the Polyurethanes Conference. SPI Polyurethanes Div, 26–29 September 1995, p. 353.
[5] Lidy WA, Rightor E, Heaney M, Davis B, Latham L, Barnes G. Proceedings of the SPI/ISOPA Polyurethanes World Congress ’97. 1997, p. 95.
[6] Neff R, Adedeji A, Macosko CW, Ryan AJ. J Polym Sci: Part B: Polym Phys 1998;36:573.
[7] Ade H, Smith AP, Cameron S, Cieslinski R, Mitchell G, Hsiao B, Rightor E. Polymer 1995;36:1843.
[8] Ade H. North Carolina State University, personal communication, 30 March 1998.
[9] Moreland JC, Wilkes GL, Turner RB. J Appl Polym Sci 1991;43:801.
[10] Seymour RW, Allegrezza AE, Cooper SL. Macromolecules 1973;6:896.
[11] Moreland JC, Wilkes GL, Turner RB. J Appl Polym Sci 1994;52:549.
[12] Moreland JC, Wilkes GL, Turner RB. J Appl Polym Sci 1994;52:569.
[13] Dounis DV, Moreland JC, Wilkes GL, Dillard DA, Turner RB. J Appl Polym Sci 1993;50:293.
[14] Turner RB, Spell HL, Wilkes GL. Proceedings of the SPI 28th Annual Technical/Marketing Conference, 1984, p. 244.
[15] Dounis DV, Wilkes GL. J Appl Polym Sci 1997;65:525.
[16] Moreland JC, Wilkes GL, Turner RB, Rightor EG. J Appl Polym Sci 1994;52:1459.
[17] Moreland JC, Wilkes GL, Moreland CG, Sankar SS, Stejskal EO, Turner RB. J Appl Polym Sci 1994;52:1175.
[18] Rossmy GR, Kollmeier HJ, Lidy W, Schator H, Wiemann M. J Cell Plast 1977;13:26.
[19] Rossmy GR, Lidy W, Schator H, Wiemann M, Kollmeier HJ. J Cell Plast 1979;15:276.
[20] Rossmy GR, Kollmeier HJ, Lidy W, Schator H, Wiemann M. J Cell Plast 1981;17:319.

[21] Elwell MJ, Ryan AJ, Grünbauer HJ M, Van Lieshout HC. Macromolecules 1996;29:2960.
[22] Yasunaga K, Neff RA, Zhang XD, Macosko CW. J Cell Plast 1996;32:427.
[23] Weier A. Goldschmidt AG, personal communication, 7 January 1999.
[24] McClusky JV, Priester Jr. RD, O'Neill RE, Willkomm WR, Heaney MD, Capel MA. J Cell Plast 1994;30:338.
[25] Magonov SN, Elings V, Whangbo M-H. Surf Sci 1997;375:L385.
[26] McLean RS, Sauer BB. Macromolecules 1997;30:8314.
[27] Rossmy GR. Progr Colloid Polym Sci 1998;111:17.
[28] Wilkes GL, Abouzahr A, Radovich D. J Cell Plast 1983;July/August:250.
[29] Tyagi D, McGrath JE, Wilkes GL. Polym Engng Sci 1986;26:1371.
[30] Nanoscope III Command Reference Manual. Update Version 4.10, Digital Instruments Nanoscope Scanning Probe Microscopes. 10 August 1995, p. 12.52–12.60.